Geochemistry Geophysics Geosystems G3

Article
Volume 12, Number 6
24 June 2011
Q05S32, doi:10.1029/2010GC003401
ISSN: 1525-2027

Published by AGU and the Geochemical Society

Submarine slope failures along the convergent continental margin of the Middle America Trench

Rieka Harders
SFB 574, Leibniz-Institut für Meereswissenschaften an der Universität Kiel (IFM-GEOMAR), Wischhofstrasse 1-3, D-24148 Kiel, Germany (rharders@ifm-geomar.de)

César R. Ranero
Barcelona Center for Subsurface Imaging, ICREA, Instituto de Ciencias del Mar, CSIC, Pg. Marítim de la Barceloneta 37-49, E-08003 Barcelona, Spain (cranero@icm.csic.es)

Wilhelm Weinrebe and Jan H. Behrmann
SFB 574, Leibniz-Institut für Meereswissenschaften an der Universität Kiel (IFM-GEOMAR), Wischhofstrasse 1-3, D-24148 Kiel, Germany (wweinrebe@ifm-geomar.de; jbehrmann@ifm-geomar.de)

[1] We present the first comprehensive study of mass wasting processes in the continental slope of a convergent margin of a subduction zone where tectonic processes are dominated by subduction erosion. We have used multibeam bathymetry along ~1300 km of the Middle America Trench of the Central America Subduction Zone and deep-towed side-scan sonar data. We found abundant evidence of large-scale slope failures that were mostly previously unmapped. The features are classified into a variety of slope failure types, creating an inventory of 147 slope failure structures. Their type distribution and abundance define a segmentation of the continental slope in six sectors. The segmentation in slope stability processes does not appear to be related to slope preconditioning due to changes in physical properties of sediment, presence/absence of gas hydrates, or apparent changes in the hydrogeological system. The segmentation appears to be better explained by changes in slope preconditioning due to variations in tectonic processes. The region is an optimal setting to study how tectonic processes related to variations in intensity of subduction erosion and changes in relief of the underthrusting plate affect mass wasting processes of the continental slope. The largest slope failures occur offshore Costa Rica. There, subducting ridges and seamounts produce failures with up to hundreds of meters high headwalls, with detachment planes that penetrate deep into the continental margin, in some cases reaching the plate boundary. Offshore northern Costa Rica a smooth oceanic seafloor underthrusts the least disturbed continental slope. Offshore Nicaragua, the ocean plate is ornamented with smaller seamounts and horst and graben topography of variable intensity. Here mass wasting structures are numerous and comparatively smaller, but when combined, they affect a large part of the margin segment. Farther north, offshore El Salvador and Guatemala the downgoing plate has no large seamounts but well-defined horst and graben topography. Off El Salvador slope failure is least developed and mainly occurs in the uppermost continental slope at canyon walls. Off Guatemala mass wasting is abundant and possibly related to normal faulting across the slope. Collapse in the wake of subducting ocean plate topography is a likely failure trigger of slumps. Rapid oversteepening above subducting relief may trigger translational slides in the middle Nicaraguan upper Costa Rican slope. Earthquake shaking may be a trigger, but we interpret that slope failure rate is lower than recurrence time of large earthquakes in the region. Generally, our analysis indicates that the importance of mass wasting processes in the evolution of margins dominated by subduction erosion and its role in sediment dynamics may have been previously underestimated.

Components: 11,500 words, 18 figures, 1 table.

Keywords: convergent margin; landslides; slope failure; subduction erosion; submarine mass wasting; tectonics.

Index Terms: 3060 Marine Geology and Geophysics: Subduction zone processes (1031, 3613, 8170, 8413); 3070 Marine Geology and Geophysics: Submarine landslides.

Received 18 October 2010; **Accepted** 12 April 2011; **Published** 24 June 2011.

Harders, R., C. R. Ranero, W. Weinrebe, and J. H. Behrmann (2011), Submarine slope failures along the convergent continental margin of the Middle America Trench, *Geochem. Geophys. Geosyst.*, *12*, Q05S32, doi:10.1029/2010GC003401.

Theme: Central American Subduction System
Guest Editors: G. Alvarado, K. Hoernle, and E. Silver

1. Introduction

[2] Submarine landslides are a geohazard that threatens life, property near or at the seashore, and industrial investments offshore. Tsunamis generated by submarine landslides strike populated coastlines, like off Papua New Guinea at the Sissano Lagoon in 1998 [*Tappin et al.*, 2001], and can destroy offshore infrastructures [e.g., *Fine et al.*, 2005]. To evaluate their occurrence and advance a global understanding of the generation of submarine mass movements, the style, size, frequency, and relation to underlying tectonic and hydrogeological processes need to be studied.

[3] Large-scale studies of different tectonic settings are important to understand how tectonic and sedimentary processes relate potential regional preconditioning factors, and trigger mechanisms for slope instability. Here we present a comprehensive inventory of mass wasting structures along more than 1300 km of the convergent margin of the Middle America Trench (MAT), including the region studied by *von Huene et al.* [2004a] and *Hühnerbach et al.* [2005] (Figure 1). We use expanded and higher-resolution bathymetric coverage, and evaluate additional side-scan sonar data, collected in selected areas after inspection of seafloor relief maps. We describe the spatial occurrence and style of the different slope failure structures from the border of Mexico and Guatemala to southernmost Costa Rica at the border with Panama, and discuss their relation to the tectonically segmented margin, review possible preconditioning factors, and infer potential triggers.

[4] This study represents the first comprehensive study of mass wasting processes along a convergent margin that is dominated by tectonic erosion processes [*Ranero and von Huene*, 2000]. The data show that changes in style and abundance of slope failures define a segmentation along the slope of the margin (Figures 1 and 2). Similarly, different failure types typically characterize the lower, middle and upper slope sectors of every segment. We interpret that the along margin segmentation, and across slope changes reflect variations in the intensity and style of the tectonic processes related to subduction erosion. In turn, the style and intensity of tectonic erosion along the subduction zone is possibly related to a first degree to changes in volcanic construction relief (ridges and seamounts) and topography formed by bending-related deformation (horst and graben), and age of the incoming oceanic plate. The changes in character of the incoming ocean plate define a segmentation that spatially corresponds to the continental slope segmentation opposite.

1.1. Previous Work on Slope Failure at Subduction Zones

[5] Only one similarly large-scale study of mass wasting processes at a subduction zone has been previously carried out [*McAdoo et al.*, 2000]. *McAdoo et al.* [2000] investigated the accretionary prism offshore Oregon, where failures are attributed to tectonic oversteepening of the prism, and are possibly triggered by seepage forces [*Orange and Breen*, 1992]. In contrast, no previous comprehensive studies of submarine mass movements at active erosive margins exist. At erosional margins, works describe single or a few landslides, for example at the Peru margin [*von Huene et al.*, 1989], offshore Costa Rica and Nicaragua [*von Huene et al.*, 2004a; *Hühnerbach et al.*, 2005] and along the slope off New Zealand [*Kukowski et al.*, 2010]. A larger-scale investigation offshore Ecuador focused on the nature and distribution of turbiditic deposits,

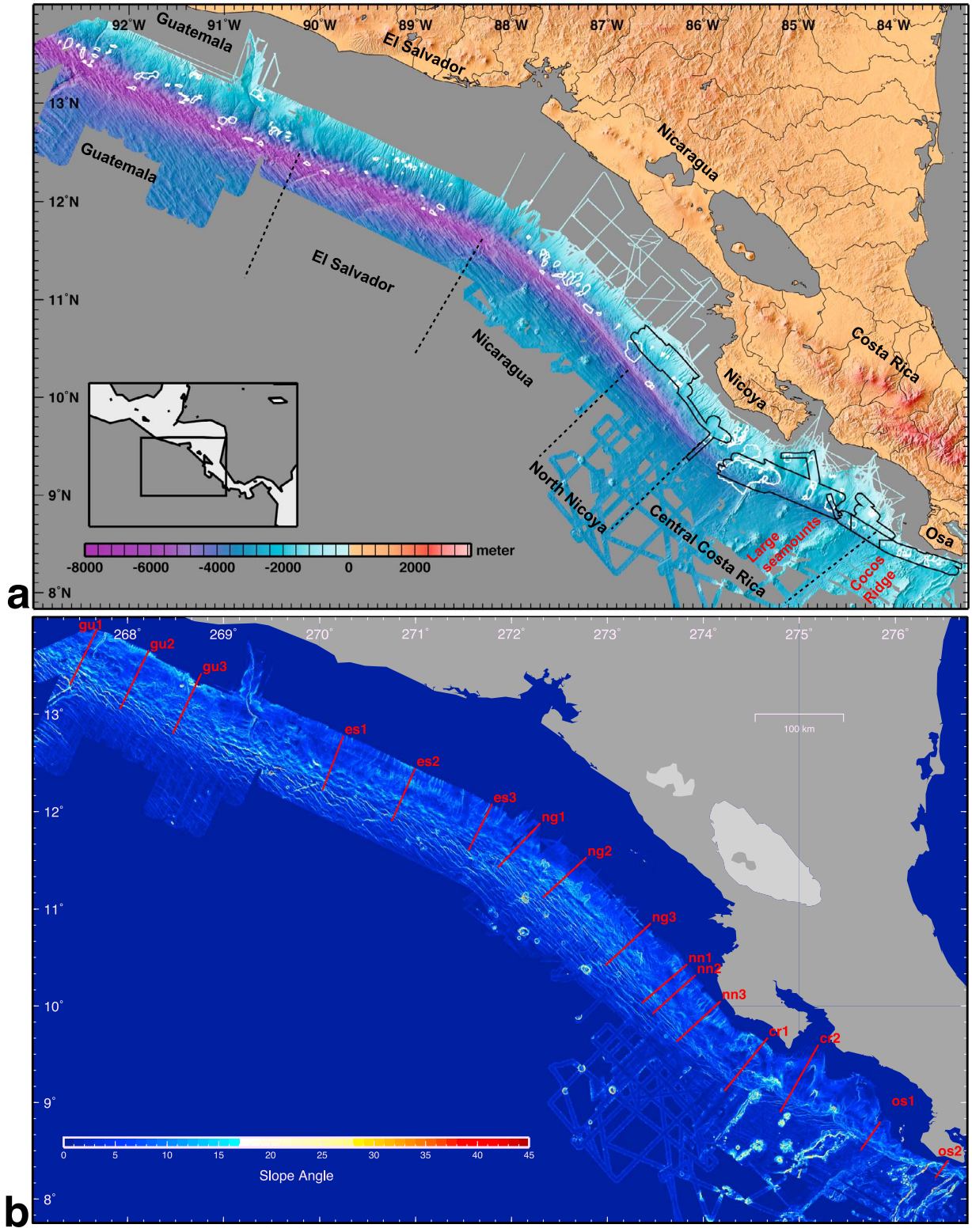

Figure 1. Data coverage along the study area of the Middle America Trench from the border of Mexico-Guatemala to the border of Costa Rica–Panama. (a) Color-coded, shaded relief digital terrain elevation of the ocean and continental plates along the MAT. The black polygons mark areas mapped with side-scan sonar. The inventory of failures includes 147 mass wasting structures (white polygons). The distribution of failures appears to be grouped in six slope segments that are delimited by black dashed lines. (b) Local slope angle used with the relief data and side-scan sonar data to map failures. Lines indicate location of profiles in Figure 2.

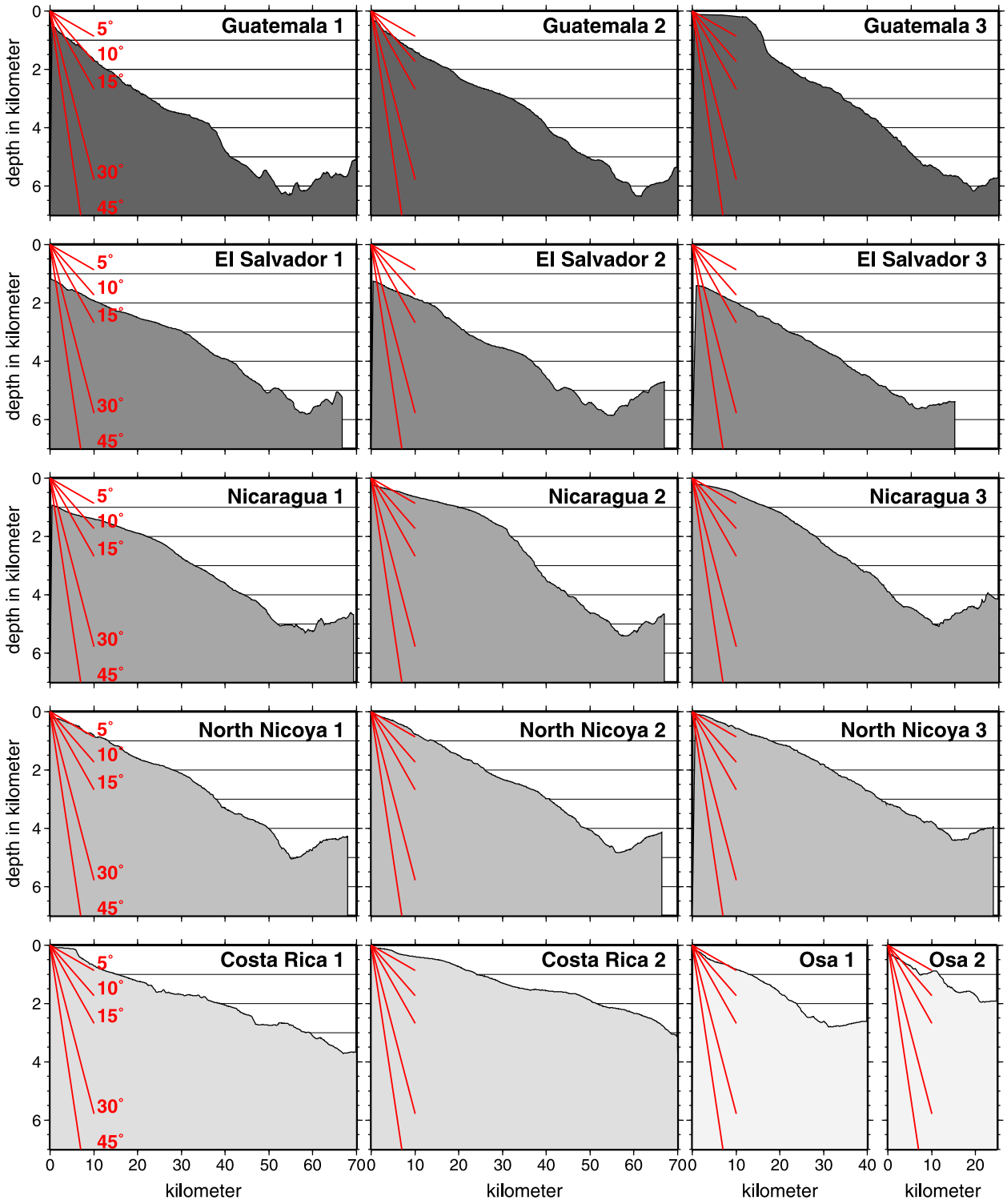

Figure 2. Selected bathymetric profiles across the different segments at representative locations to show regional slope morphology and slope dip angle (profile locations shown in Figure 1b).

but did not explicitly analyze the failure structures in the continental slope [*Ratzov et al.*, 2007].

1.2. Preconditioning and Trigger Mechanisms

[6] Preconditioning factors are those that may make areas prone to future failure, e.g., overall stress history, sediment type, grain size distribution, prior straining, degree of saturation and gas hydrate dissolution and dissociation [e.g., *Sultan et al.*, 2004]. The trigger of submarine mass movements is defined as the external stimulus that initiates slope instability [*Sultan et al.*, 2004], such as slope oversteepening, seismic loading, and storm wave loading. When occurring at exceptionally fast rates, some preconditioning factors might become triggers. Examples of these factors are very high sedimentation rates [e.g., *Sawyer et al.*, 2007], sediment underconsolidation caused by overpressures [e.g., *Flemings et al.*, 2008], overpressure generated by gas hydrate dissociation [e.g., *Mienert et al.*, 1998], groundwater sapping [*Johnson*, 1939], and factors related to glacial unloading (e.g., flexing of the crust), and rapid sedimentation of low-plasticity silts [*Locat and Lee*, 2002].

[7] Early studies along the MAT recognized signs of slope mass wasting offshore Guatemala and Costa Rica [*Aubouin et al.*, 1982; *Baltuck et al.*, 1985] but were based on geographically restricted data sets. The only investigations on mass wasting of regional significance have been carried out offshore central Costa Rica and a slope section offshore Nicaragua with limited bathymetric, seismic reflection data [*von Huene et al.*, 2004a], and in the same Costa Rica area with side-scan sonar data [*Hühnerbach et al.*, 2005]. *von Huene et al.* [2004a] showed how subduction of large seamounts in Costa Rica deforms the slope sediment and basement (the so-called margin wedge), causing large rotational slumps with deep-seated slide planes, the largest of which were possibly tsunamigenic [*von Huene et al.*, 2004a]. They also show that a sector of the Nicaragua slope contains translational slides, of uncertain origin, some of which might be related to a liquefaction phenomenon at intercalated ash layers [*Harders et al.*, 2010].

1.3. Tectonic Setting of the Active Erosive Margin of Middle America

[8] The convergent margin of the MAT is dominated by tectonic erosion processes. Evidence for tectonic erosion during much of Neogene time has been found at the Guatemala [*Vannucchi et al.*, 2004], Nicaragua [*Ranero et al.*, 2000] and Costa Rica [*Ranero and von Huene*, 2000; *Vannucchi et al.*, 2003] segments of the margin. Basal subduction erosion removes material from the underside of the overriding plate causing a progressive oversteepening of the continental slope. Frontal subduction erosion is a direct consequence of subducting ocean plate relief and slope failure. Both processes control the architecture of the margin created by long-term tectonics [*Ranero et al.*, 2008]. Related to subduction erosion the continental margin undergoes (1) fracturing and pronounced, spatially localized and temporally limited, uplift and oversteepening above subducting seamounts, ridges and large horsts of the underthrusting plate; (2) widespread extensional faulting subparallel to the trench axis; and (3) gradual slope oversteepening. All three processes favor occurrence of mass-wasting phenomena along these types of margins. About 85 km of oceanic plate are subducted per million years at current convergence rates [*DeMets et al.*, 1990], thus numerous seamounts, grabens and ridges underthrust the overriding plate in that time. This implies that most landslide scars and mass wasting deposits on the lower continental slope are rapidly modified by tectonics and the structures mapped in this study are possibly not older than several hundred thousand years. The preservation potential of slides at passive margins, or active margins with accretionary prisms is likely higher as these do not undergo continuous modification of surface and deep structures, except at those where a exceptionally high sediment input and related frequent failures overprint older features.

2. Methods

2.1. Seafloor Mapping

[9] Multibeam bathymetric data along the MAT were collected during German R/V *Sonne* cruises SO76, 81, 107, 144 legs 1 and 2, 150, 163 leg 1, and U.S. R/V *Maurice Ewing* cruises 0005 and 0104 using the Atlas Hydrosweep system and, *Sonne* 173 leg 2 cruise using the Kongsberg Simrad EM-120 system. Water velocity profiles were calculated from CTD measurements conducted during most of these cruises. The bathymetric data were cleaned and converted to depth soundings with the MB system [*Caress and Chayes*, 1996] and gridded with GMT [*Wessel and Smith*, 1998] at 0.001° node spacing [*Ranero et al.*, 2005]. Side-scan sonar data were collected along most of the Costa Rica slope and a segment off Nicaragua with the "towed ocean bottom instrument system" (TOBI system) during

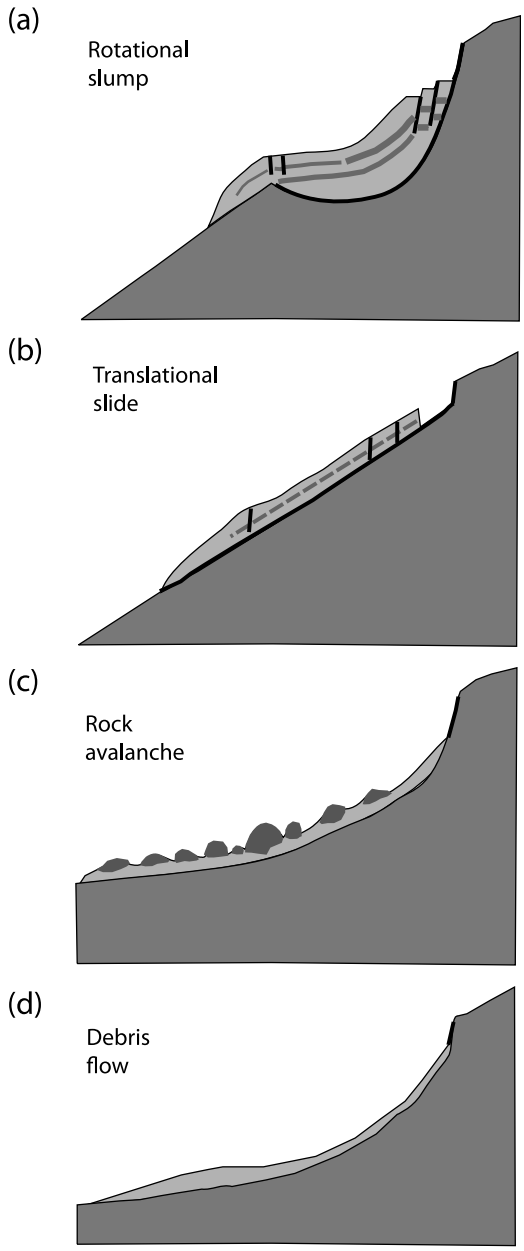

Figure 3. Conceptual cartoons of a cross section of submarine (a) rotational slump; (b) translational slide; (c) rock avalanche, a cohesionless slump with deposits containing large blocks; and (d) debris flow, cohesionless plastic flow containing boulders.

Sonne cruises 163, 144 and the "deep-towed side-scan sonar system" (DTS-1) during *Sonne* 173 [*Bialas et al.*, 1999; *Weinrebe and Flueh*, 2002; *Weinrebe and Ranero*, 2004; *Hühnerbach et al.*, 2005; *Sahling et al.*, 2008].

[10] Our inventory includes only failure structures with clear headwall scarps and flanking sidewalls. The horizontal resolution of the bathymetry allowed for the identification of landslides scars with dimensions of >0.5 km length, and >1 km width. The minimum height of vertical features, like headwalls, that could be indentified is >20–40 m high. Smaller features have been locally observed but they are not well defined along the margin segments and thus were not included in the inventory. In general, resolution of the bathymetric grids is higher in the shallower areas of the upper slope due to data redundancy and higher accuracy of water depth measurement, with net resolution also depending on coverage.

2.2. Classification and Terminology

[11] In this work we use the term landslide, mass wasting structure and slope failure as general terms, not implying specific mechanisms, whereas the terms "translational" slide and "rotational" slump imply a failure mechanism (Figure 3).

[12] We use the classification of *Hampton and Lee* [1996], as well as that of *Mulder and Cochonat* [1996] even though the "cohesion" of the failed material that is used to define the terms "translational slide" and "rotational slump" is often unclear in our study, as there was often no identifiable failure deposits. However, we think that we can use these classification schemes to characterize the mapped mass wasting structures on the fore arc: Rotational slumps are defined by a scoop-shaped slide plane, relatively short runout distances and relatively high headwalls. Translational slides with strata parallel slide planes display relatively long runout distances, in relation to their headwall heights. Rock avalanches display a cohesionless slump with deposits containing large blocks (Figure 3). Debris flows are cohesionless plastic flows containing boulders. Creep is defined as slow sediment deformation that does not result in a clear headwall, sidewalls or an exposed slide plane. Instead the seafloor shows wavy sediment features such as compressional ridges that are generated by slow, downslope movements of the sediment.

[13] We additionally use the Skempton ratio (max. headwall height to slide length ratio) to constrain the translational or rotational character of the slide or slump, if the failure plane does not show either a clear rotational or translational character. Ratios <0.15 define a translational slide and ratios >0.33 define a rotational slump [*Skempton and Hutchinson*, 1969]. Many failures in our study have a translational slide plane but are disintegrative and lack visible deposits outside the scar area. In those cases, only the scar with a headwall and sidewall could be

Table 1. Main Characteristics Defining the Segments of the Continental Slope[a]

Segment	Failure Mode			Continental Slope		Main Preconditioning Mechanism
	Upper Slope	Midslope	Lower Slope	Width (km), Minimum–Maximum, Average	Dip Angle (deg), Minimum–Maximum, Average	
Cocos Ridge–Osa Peninsula		RA, SP	RA, SP	6.5–20, 8	6–20, 8	Regional oversteepening by tectonic erosion. Fractures by ridge relief.
Seamounts–Central Costa Rica	SD	RA, SP	RA, SP	44–73, 56	2.5–4.5, 3.5	Local oversteepening and fractures by uplift by subducting seamounts.
North Nicoya		SD	SP	52–55, 53	4.5–4.7, 4.6	Ash layers.
Nicaragua		SD	SP	43–51, 48	4.6–5.6, 5.1	Oversteepening, regionally by tectonic erosion and locally by seamounts. Normal faults. Ash layer.
El Salvador	SD		SP	49–57, 52	3.6–4.7, 4.4	Oversteepening by canyon erosion.
Guatemala	SD	SP	SP	49–64, 55	4.8–6.1, 5.3	Oversteepening by tectonic erosion. Normal faults.

[a]RA, rock avalanche; SP, slump; SD, slide. Slope dip angle has been estimated from profiles of the entire width of the slope.

detected, and, therefore (under our scheme of classification) the runout distances are limited to the scar toe and represent only minimum distances. Lacking visible runout distances of the landslides makes comparisons with mass wasting structures of other margins more difficult, as the full information of dimension and the dynamic rheology (often inferred from the Skempton ratios) are not well constrained by that method here. Nevertheless, in our study morphologies of slide scars indicating translational character have Skempton ratios that fall into the translation type of slide, even when deposits could not be included in the measurement.

3. Results: Segmentation of Distribution of Slope Failures

[14] Using multibeam bathymetry from Guatemala to Panama and deep-towed side-scan sonar data from the continental slope of Nicaragua and Costa Rica we mapped 147 mass wasting structures that fall within 5 main failure types (rotational slump, translational slide, rock avalanche, debris flow, and creep) (Figure 1). Within these 5 main failure types we found that the prevailing styles of failure plane and deposits are different in several areas of the margin. We found that failure distribution displays a partitioning in six slope segments visible in their map distribution (Figure 1).

[15] The segmentation of the slope (Figure 1) is apparent when average slope dip and width (Figure 2), dominant failure mode, and failure abundance are compared (Table 1). Interestingly, a segmentation with similar dimensions occurs in the character of the ocean plate. The slope of the Cocos Ridge–Osa Peninsula segment contains mainly slumps and rock avalanches in the lower-middle slope. These failures are related to the subduction of sharp crests over the broad Cocos ridge (Figure 1 and Table 1). The Seamounts–Central Costa Rica segment shows rotational slumps and large scars caused by underthrusting of large seamounts. The North Nicoya segment is defined by a decrease in slope failure occurrence, and a few, comparatively small translational events characterize the segment. Here, the ocean plate is the smoothest along the trench (Figure 1 and Table 1). A transition leads to the Nicaragua segment, characterized by abundant, large translational slides, and an ocean plate containing abundant small seamounts and trench axis–parallel horst and graben relief. El Salvador segment is defined by a stable lower and middle slope, and abundant, small translational slides in the upper

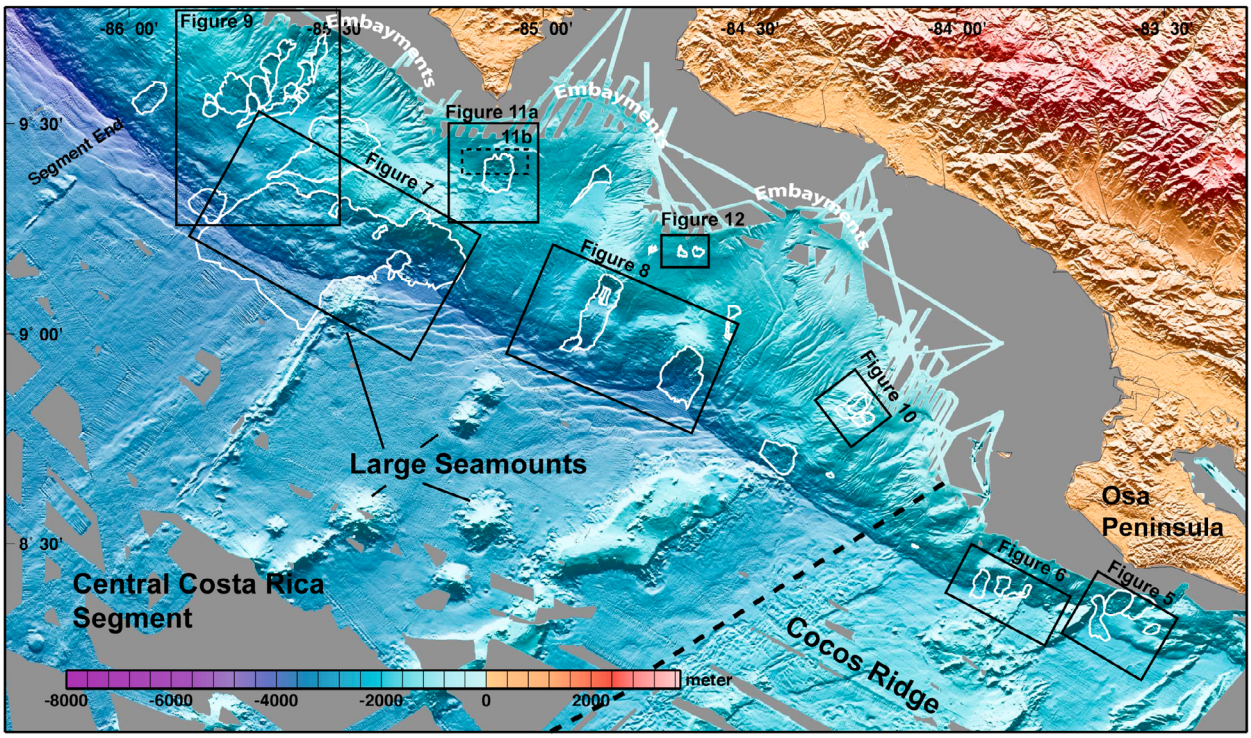

Figure 4. Seamounts–Central Costa Rica segment and Cocos Ridge–Osa Peninsula segment. The incoming plate of the segment is separated into a seamount-dominated and a ridge-dominated region. Failures in the slope also show a relation to the incoming plate relief domains. The margins display rotational slumps and scars from seamount subduction. Close-ups of representative structures and their interpretations are shown in Figures 5–12 as marked by the black boxes.

slope. Here the plate lacks seamounts and horst and grabens strike oblique to the trench. The Guatemala segment is dominated by abundant, comparatively small slumps across the lower-middle slope and a hummocky slope terrain. The ocean plate displays the most pronounced horst and graben relief.

3.1. Cocos Ridge–Osa Peninsula Segment

[16] The southernmost segment boundary is marked by data coverage. The north boundary is delineated by the outcrops of the Cocos Ridge crust. Here 1.0–1.5 km high crests ornamenting the broad, elevated topography of Cocos Ridge collide with the continent (Figure 4). The slope is narrow and steep with an average width of 8 km and angles of 6°–20° (Table 1 and Figure 2).

[17] Offshore Osa Peninsula (Figures 1 and 4) the >100 km wide Cocos Ridge is subducting. The ridge forms a 1.5 km high swell, with local seafloor relief 0.5–1 km high [*von Huene et al.*, 2000]. We mapped previously unidentified rotational slumps and associated rock avalanches caused by subduction of local ridges (Figures 4, 5, and 6). A subducting ridge crest with steep flanks caused the Sirena slump (Figure 5), with the failed material deposited along the southern steeper flank. The headwall height is 1000 m, with maximum slope angle of 51° in the uppermost part and 30° in the lower part. The length of transport of the deposits is visible, with the front of the failed mass forming a tongue shaped toe (Figure 5). The runout distance is 12 km, yielding a Skempton ratio of 0.006, indicating its translational character, although the steep failure plane has characteristics of a submarine slump or rockfall with rock avalanche deposits. Similar slumps linked to ridge subduction occur in the vicinity farther northwest (Figures 4 and 6), and indications of ongoing fracturing of the overriding plate are abundant (Figure 6).

3.2. Seamounts–Central Costa Rica Segment

[18] The northwestern limit is marked by a ridge in the oceanic plate that projects landward to a cohesive slump in the lower slope (Figures 1 and 4).

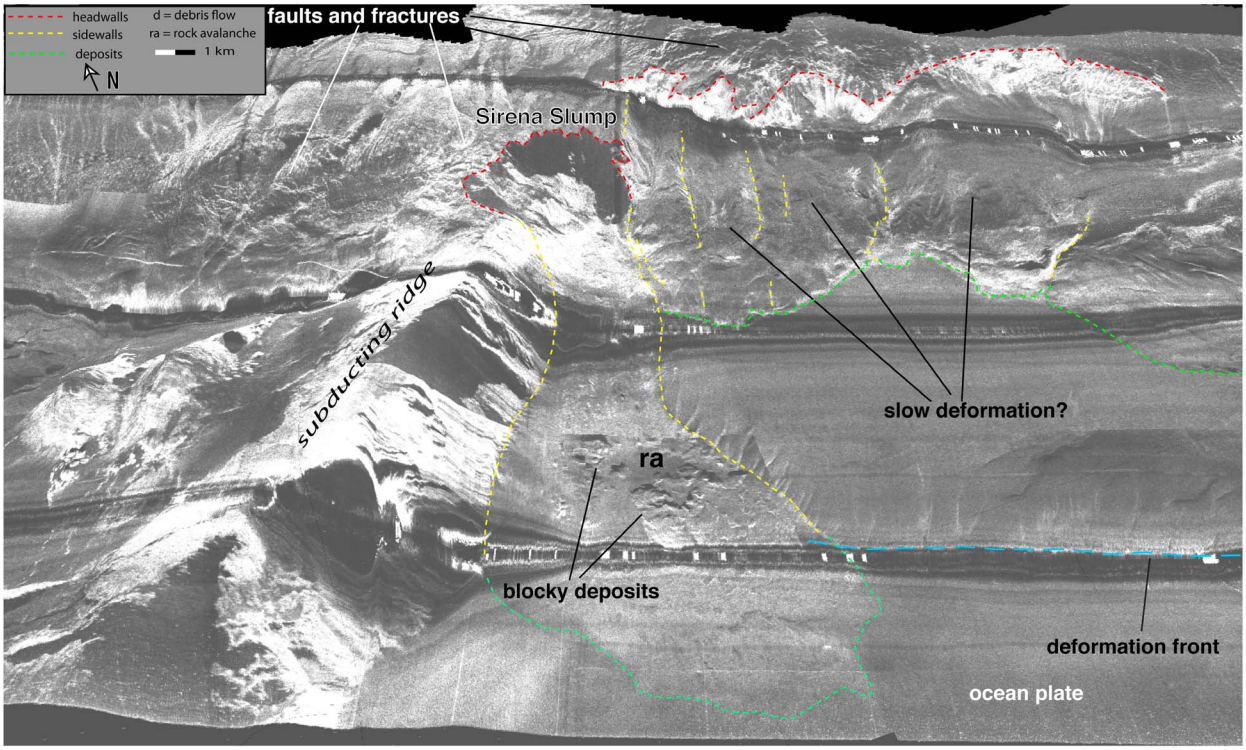

Figure 5. Perspective view of side-scan sonar imagery draped on multibeam bathymetry of the Sirena slump in the lower slope offshore Osa Peninsula and associated runout deposits, including large blocks, that reach the ocean plate (location in Figure 4). The slope scar is 12 km wide, with a 1 km high headwall that dips 30°–51°. The avalanche is related to subduction of a sharp ridge, cresting Cocos Ridge, clearly visible in the images. Southeast of the scar, high-backscatter slope-subparallel structures may be incipient headwalls (marked in red). Downslope of them, tongue-shaped bodies bounded by slope-normal structures (marked in yellow) might indicate developing gravity-related deformation.

Seamounts cover 40% of the oceanic plate and reach up to 4 km height and 40 km width [*von Huene et al.*, 2000]. The continental slope opposite displays geomorphic features generated by tectonic erosion [*von Huene et al.*, 2000], local reentries at the slope toe where seamounts have collided with the margin, slope grooves along seamount subduction paths, and rotational slumps (Figure 4). Large-scale (>20 km long or wide) rotational slumps and rock avalanches occurring in the lower and middle slope characterize this segment. Mean slope angles are 2°–5°, i.e., lower than at other segments (Table 1). However, the slope is locally uplifted to 20°, although headwall scarps are steeper (Figures 1b and 2). In contrast to other segments, the slope deformation of this segment has been relatively well studied before [*von Huene et al.*, 2000; *Ranero and von Huene*, 2000; *von Huene et al.*, 2004a, 2004b]. The seamounts, created by the Galapagos hot spot, have been subducted here for at least 300,000 years assuming a current convergence rates [*Werner et al.*, 1999; *von Huene et al.*, 2000], and most slope failures are probably related to that process.

3.2.1. Rotational Slumps

[19] Owing to their large dimensions most slumps and scars within this segment have been previously identified [*von Huene et al.*, 2000, 2004a]. Here we add and interpret new information based on the increased resolution bathymetry from about 200 to 100 m grid, and unpublished side-scan sonar data.

[20] The largest failure is the rotational Nicoya slump (Figures 4 and 7). The slump block is 35 km long and 60 km wide [*von Huene et al.*, 2004a]. Seismic profiles show its deep-rooted rotational slide plane, affecting the entire thickness of the overriding plate [*von Huene et al.*, 2004a]. Surface expressions of the slump include debris flows (d), debris avalanches (da) and rock avalanches (ra) (Figure 7). The headwall height increases from

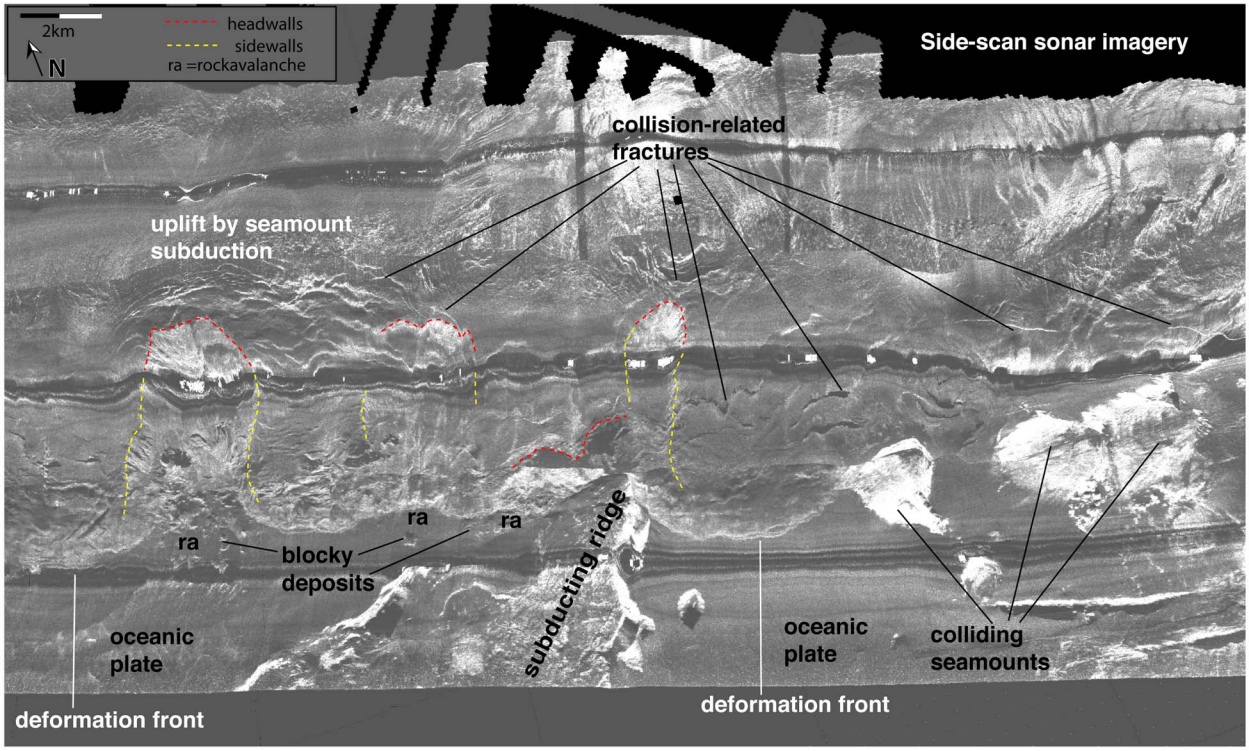

Figure 6. Perspective view of side-scan sonar imagery draped on multibeam bathymetry of the deformation and slope failures caused by ridges and associated seamount groups on the Cocos Ridge in the fore arc SW of Osa Peninsula (location in Figure 4). Numerous slope-parallel fractures in the slope occur upslope of the headwalls of slumps. Apparently, failures are disintegrative slumps that develop into rock avalanches.

350 m in the north up to 1000 m in the south. We infer that the dimensions of the Nicoya slump are caused by slumping of the fore arc over two subducting seamounts located both at about the same distance from the trench axis. We propose that in addition to a seamount described in previous papers located under the Rio Bongo uplift, there is a smaller subducting seamount to the northwest, and that sliding of the entire overriding plate over the flanks of the seamounts caused a structural modification of the rotational slump (Figure 7). This can be inferred from morphology, which consists of a relatively shallow and continuous headwall, and a slide plane along the plate boundary fault (i.e., <5°) imaged in seismic data [*von Huene et al.*, 2004a, Figure 2], and a 0.07 low Skempton ratio. The larger seamount in the southeast has caused a more disintegrative rotational part of the slump.

[21] Farther southeast is Jaco scar, a large slump caused by an underthrusting seamount that has left during the past ~300.000 years a 27 km long trace of slumped rock masses filling a furrow (Figure 8). The furrow sidewall scars can be traced to the deformation front. The most recent slump is at least 20 km long and 5 km wide, containing blocky deposits that traveled up to 17 km. The rotational failure plane has a ~1000 m high headwall, with an angle of up to 40°. Parrita scar located to the southeast (Figure 8) is a slump similar in size, shape, and a seamount-related furrow.

3.2.2. Translational Slides

[22] In this segment translational sliding style changes depending on slope morphology and failure location on the upper, middle or lower slope.

3.2.2.1. Slides With Planar Body Deposits

[23] Areas where high-topography features have repeatedly subducted display embayments (Figure 4) attributed to thinning by tectonic erosion [*Ranero and von Huene*, 2000]. Three embayments occur from Nicoya Peninsula to northwest of Osa Peninsula [*von Huene et al.*, 2000] (Figure 4). A series of overlapping scars on the steep flank of the northernmost embayment indicate successive, retrogressive translational slides (retrogressive means that other slides are induced above the original one,

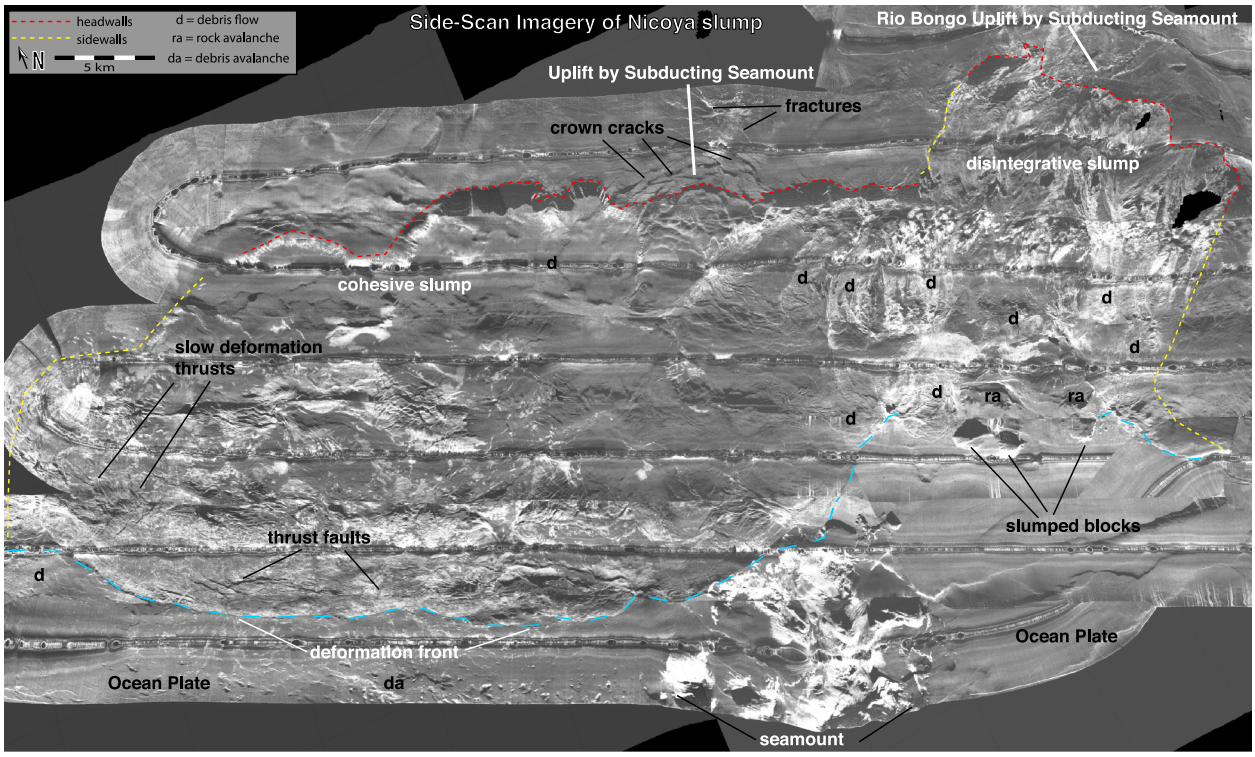

Figure 7. Side-scan sonar imagery of the region of Nicoya slump (location in Figure 4). The complex morphology of the >60 km wide slump probably developed when the slope failed over two subducting seamounts. A large seamount is located in the SE causing the Rio Bongo uplift, and a smaller seamount is located under the headwall near the middle region of the slump structure, indicated by crown-shaped cracks and associated fractures. The headwall and deposits of the northwestern part of the slump differ from the morphology of the slump in its southeastern area. Blocky deposits and high headwalls represent a slump with a disintegrative character that developed rock avalanches in the southeast, downslope of the Rio Bongo uplift. The northwestern two thirds of the slump shows a more cohesive translational character. Abbreviations are as follows: d, debris flow; da, debris avalanche; ra, rock avalanche.

building similar headwalls upslope [*Mulder and Cochonat*, 1996]) (Figures 9a and 9b). The mobilized material moved downslope into the embayment floor. Some planar sediment deposits there (Figure 9a), may represent "mixed slides," defined as slides with a planar body and a shallow headwall, akin to gliding snow slabs created during snow avalanches [*Mulder and Cochonat*, 1996]. The scars of the embayment walls are ~7 km long and ~4 km wide on average, with headwalls 30–60 m high and about 18° dip angles (Figure 9b).

3.2.2.2. Slides With Coherent Deposits

[24] As subducting seamounts and ridges underthrust deeper, they uplift the upper continental slope, and produce broader uplifts that cause moderate slope oversteepening (7°–10°). There, failure type changes to moderate to large (8–10 km long, 5–7 km wide) cohesive translational slides, rather than the slumps of the middle-lower slope. An example is Quepos slide formed at a slope angle of 7.5° near the shelf break (water depth 214 m) (Figures 4 and 10). The slide is ~8 km long and 9.5 km wide, with a headwall height of 160 m, and a headwall angle of 25°. The 0.02 Skempton ratio, indicates a translational character. The deposits front created a 100 m high ridge terminating in a tongue-shaped toe that shows compressional sediment structures (Figure 10). The slide consists of at least 4 events that possibly occurred sequentially in time, caused by the progressive southeastward migration of the obliquely oriented subducting ridge (Figure 4).

[25] A similar slide is Cabo Blanco slide, possibly initiated by upper slope uplift by a subducting seamount in the prolongation of the seamount that caused the Rio Bongo uplift and participated in Nicoya slump (Figure 4). The slide is 9.8 km long, 7.3 km wide and has a maximum headwall height of 160 m. Side-scan imagery and bathymetry show a complex morphology of a failed mass in the

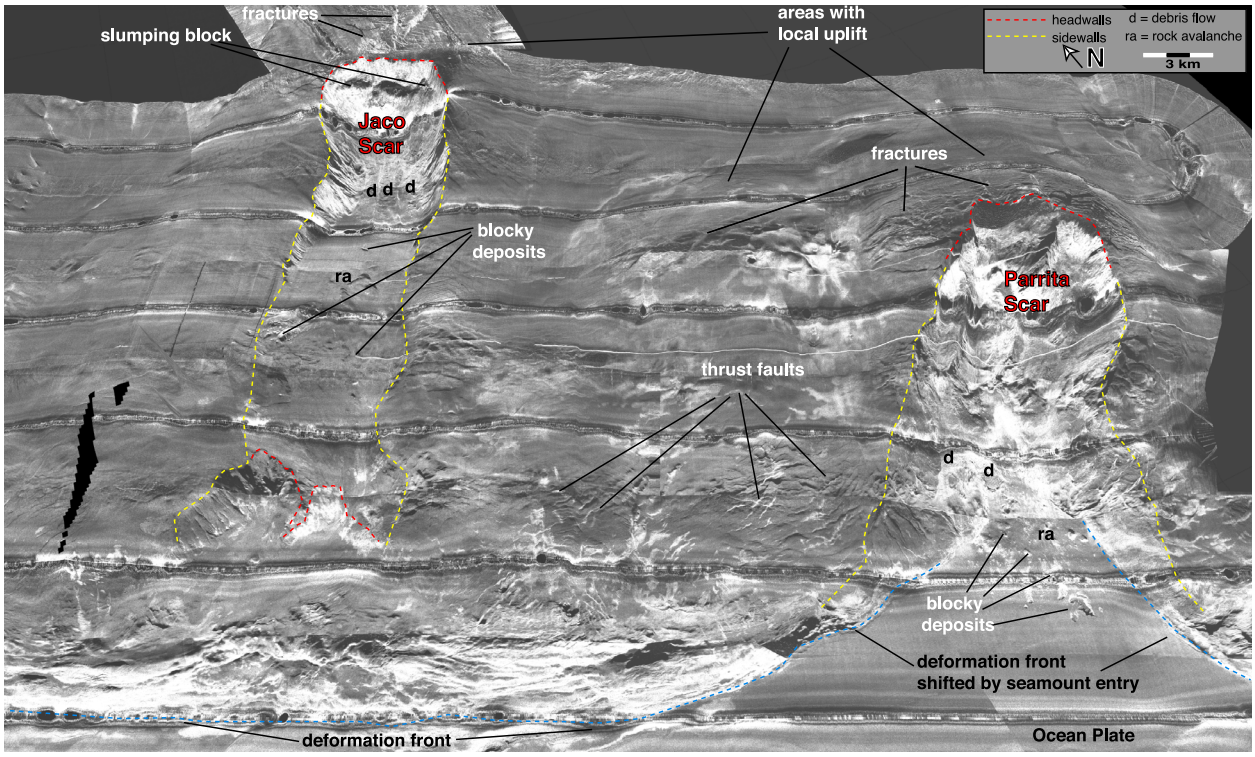

Figure 8. Perspective view of side-scan sonar imagery draped on multibeam bathymetry of the region of Costa Rica deformed by subducting seamounts. Two underthrusting seamounts are currently located under the so-called Jaco and Parrita scars (region location in Figure 4). The grooves in the slope bounded by sidewall faults mark the trajectory of the underthrusting seamounts and contain the deposits of a series of successive rotational failures produced as the seamounts subduct deeper under the overriding plate. The seamounts uplift and fracture an area considerably larger than the area that fails in their wake. Abbreviations are as follows: d, debris flow; ra, rock avalanche.

northwest that grades to slid blocks farther downslope. In the southeast, the upper region contains a partially detached block. Downslope occur a series of compressional ridges formed by a previous failure (Figures 11a and 11b).

3.2.2.3. Slides Without Visible Deposits

[26] In the uppermost slope, occur a series of comparatively small translational slides, which are not clearly related to subducting seamounts. Two of them, named the BGR and Geomar slides (Figure 12), have been studied in some detail but failure causes remain unclear [*Marquardt*, 2005]. These slides have ~40 m headwall heights and ~2 km total lengths.

3.3. North Nicoya Segment

[27] This segment occurs opposite the smoothest oceanic plate of the study area (Figures 1 and 4). The ocean plate was formed at the East Pacific Rise and it is separated from lithosphere to the south, formed at the Cocos-Nazca spreading center, by a ridge marking the paleoplate boundary (Figures 1 and 13a). The slope is smooth, with numerous normal fault scarps across the middle slope visible in bathymetry (Figures 13a and 13b) and side-scan sonar images (Figure 14). Mean slope angles of the middle slope are gentle (5–14°), increasing to 17° at the lower slope. The area contains many fewer failures than adjacent segments.

3.3.1. Translational Slides

[28] All slide scars in this segment are comparatively small and shallow, displaying translational character, typically with no visible deposits near the toe (Figures 13b and 14). The maximum slide length is 7 km, a maximum width of 3 km and maximum headwall height of ~40 m. Trench axis subparallel normal faults occur within the middle slope, where translational slides appear to start (Figure 14).

[29] A typical translational slide in this segment is Hermosa slide (Figures 13b and 14), which occurs

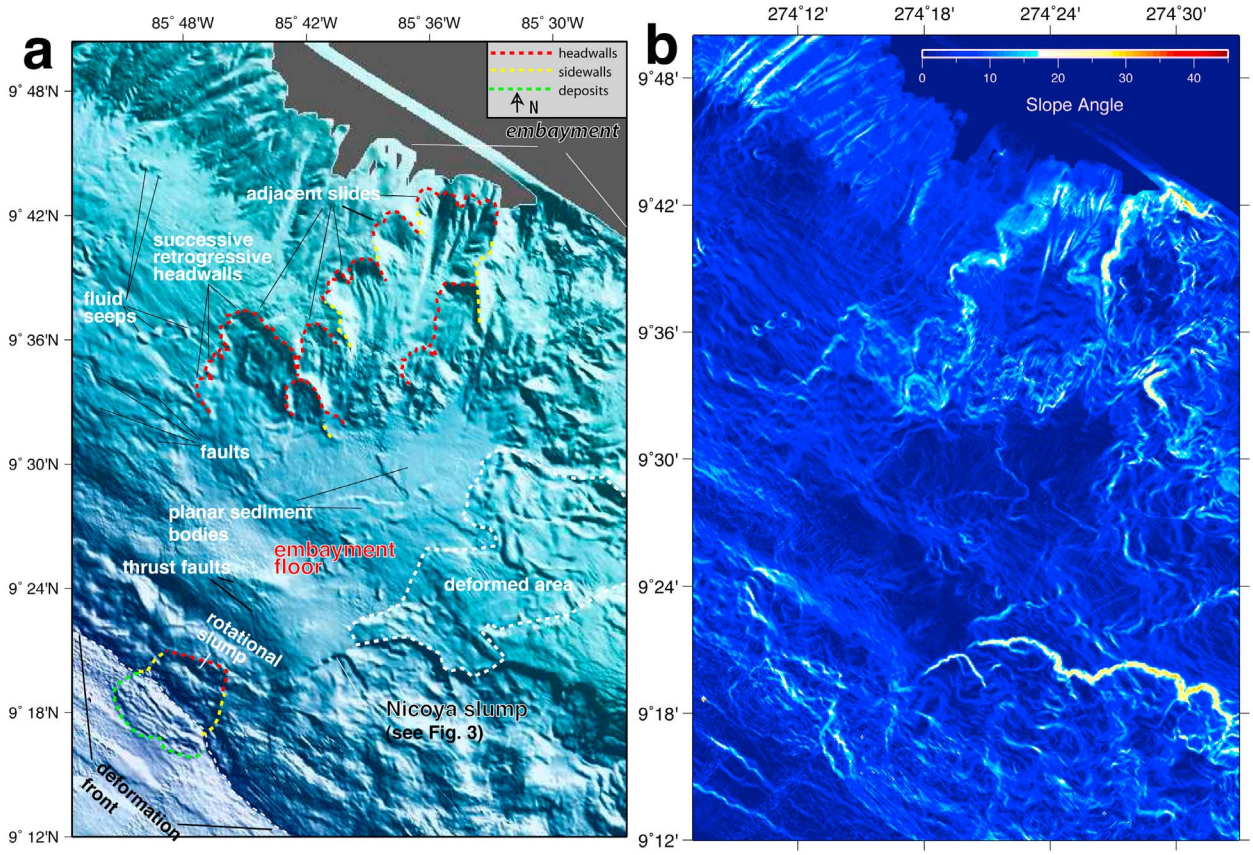

Figure 9. Northernmost embayment offshore Costa Rica. (a) Multibeam bathymetry map and (b) slope angle. The NW flank is sculptured by several headwalls and sidewalls of retrogressive translational slides. Slides developed on the inner wall of the embayment and the failed material followed canyon paths to build planar sediment bodies in the embayment floor.

together with 4 similar neighboring slides in the southeast [*Harders et al.*, 2010]. Hermosa slide occurs in 1900–2500 m water depth, with a 25 m headwall height and a 13° headwall angle. The sidewalls of the scar slightly converge toward the scar foot and can be followed about 7 km downslope, but the runout point is unclear. As for most translational slides along the MAT, the bathymetry data do not show an elevated deposition area near their toe. Side-scan sonar data of Hermosa slide show faults or fissures within failed sediment where parts form large block and sheet deposits overlying the slide plane (Figure 14).

3.3.2. Rotational Slump

[30] In the northwesternmost middle-lower slope section occurs a large (21 km wide and 22 km long) structure with hummocky morphology, containing mound structures and a slump scar in its uppermost part (Figures 15a and 15b). The structure consists of an uplifted area bounded trenchward by a well-developed 300 m high headwall, but no sidewalls occur downslope (Figures 15a and 15b). The sediments at the toe of the area show possible compressional faulting which may indicate short distance slow deformation or creep (Figure 15a). This structure is possibly related to a subducting seamount, imaged under the uplifted region in a seismic reflection profile [*McIntosh et al.*, 2007].

3.4. Nicaragua Segment

[31] This segment starts gradually where the offsets of normal faults cutting oceanic plate increase to form scarps >200–350 m high, and a series of seamounts (smaller than offshore Costa Rica) occur across the ocean plate (Figures 1 and 16). To the NW, the segment terminates where the trench axis changes strike to a NW-SE orientation, roughly coincident with a fracture zone that separates segments of the oceanic plate [*Wilson*, 1996]. Large

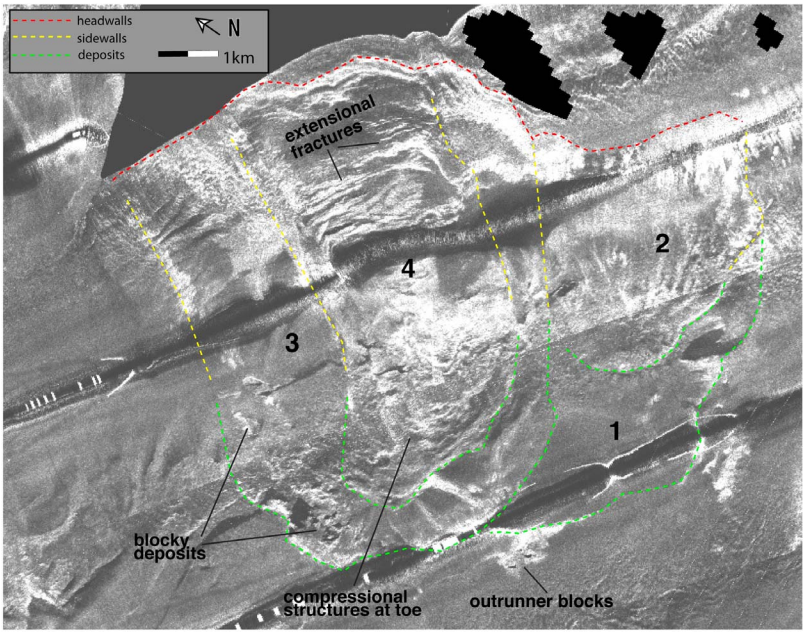

Figure 10. Perspective view of side-scan sonar imagery draped on multibeam bathymetry of the cohesive, translational Quepos slide related to uplift of the uppermost slope due to subduction of a ridge offshore central Costa Rica. Numbers 1–4 indicates four failure events that spatially overlap and possibly represent a time evolution (1 is the oldest and 4 is the youngest) in the development of the slide caused by the southeast oblique subducting of a ridge (location of region in Figure 4).

translational slides characterize this segment, and are concentrated along the middle slope with an average dip (7°–17°) steeper than in other segments (Figure 16).

3.4.1. Translational Slides

[32] Large retrogressive translational slides start along the steep upper to middle slope transition, coincident with NW trending normal faults with offsets of 50–200 m. The headwall height to length ratio of slides is typically low and reflects their translational character; even though only the slide plane length and not the full runout could be measured (Figure 16a). Slide plane dimensions range between 5 and 12 km in length and 3–7 km in width, with 50–450 m high headwalls. Scar sidewalls typically converge downslope, and the failure plane is bedding parallel, indicating that sliding probably occurred along a weak layer of stratified sediment. Many slides show slide blocks overlying the slide plane with a characteristic hummocky surface (Figures 16b and 16c). Near slide toes, where slide scars narrow, a channel occurs in some cases, which may have been incised by turbidity currents. Most slide scars disappear at the transition from middle to lower slope, where gradients decreases over 4–5 km, to give way to an increase up to 12° at the slope toe.

[33] A typical example of translational slide is the Masaya slide (Figure 16b). The slide starts in 1700 m water depth on the 8°–12° dip upper to middle slope. The headwall is up to 160 m high, with a 28° maximum dip. The main scar is 18 km long, up to 6.2 km wide and narrows to <2 km at its lower end. No deposits are visible downslope, but a channel at its toe may indicate disintegration of the slide into turbidites (Figure 16b).

3.4.2. Rotational Slumps

[34] Irregularly shaped rotational slumps are uncommon on the Nicaragua segment, but some occur at the low-angle transition from middle to lower slope (Figure 16d). In contrast to translational slides, these slumps show wide headwalls and short sidewalls. Dimensions are ~3 km in length, ~10 km in width and up to 200 m headwall heights.

3.5. El Salvador Segment

[35] Its SE border is marked by a change in strike of the MAT, and a fracture zone in the oceanic plate (Figures 1 and 17a). The northwestern bound-

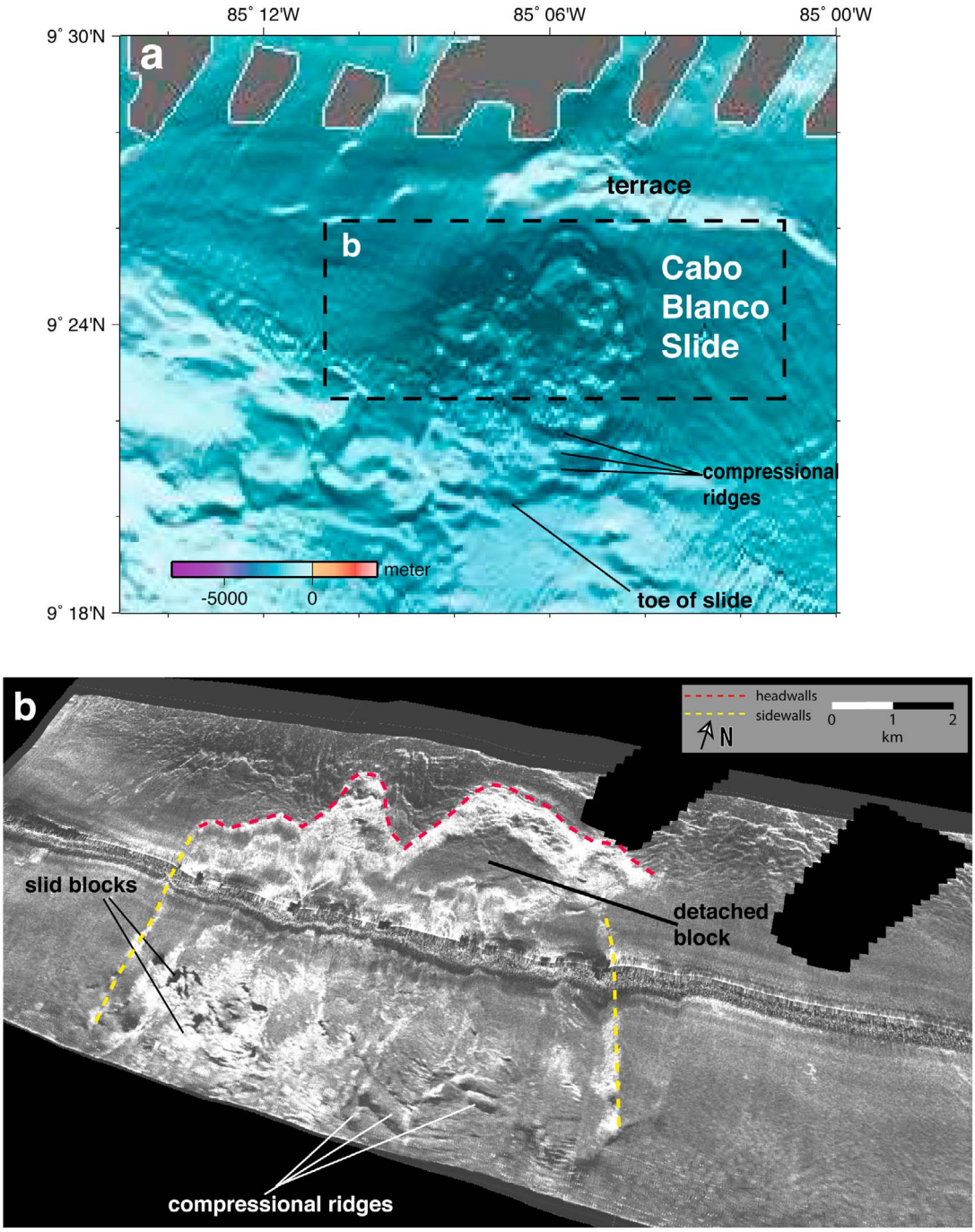

Figure 11. The Cabo Blanco slide, related to uplift of the uppermost slope due to subduction of a seamount, located southeast of Nicoya Peninsula. (a) Shaded relief bathymetric map (location of region in Figure 4). (b) Perspective view of side-scan sonar imagery draped on multibeam bathymetry of the upper portion of Cabo Blanco slide. Location of Figure 9b is marked in Figure 9a. The slide is a cohesive, translational type with detached, coherent blocks in the upper area, slid blocks in the middle portion, and compressional ridges in the lower segment.

ary is gradual, with no sharp change in the fabric of the ocean plate, but with an increase in failures in the middle slope (Figure 1).

[36] The El Salvador segment has few failure-related structures (Figure 17). Only small translational slides occur on the uppermost slope at the segment center. Similarly to the Nicaragua segment,

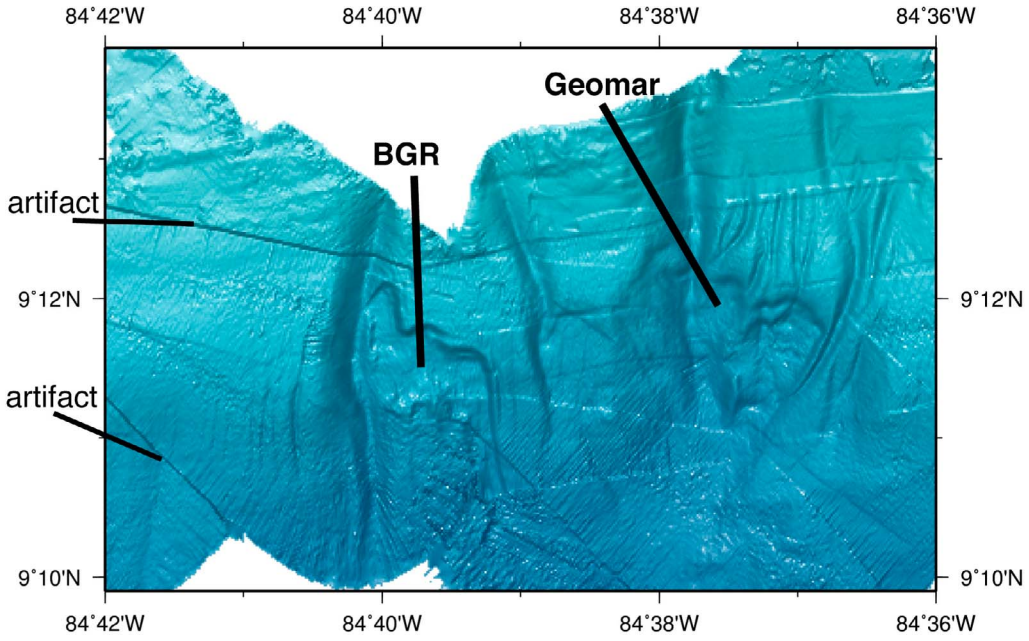

Figure 12. Shaded relief bathymetric map of the BGR and Geomar slides located in the uppermost slope offshore Costa Rica. The scars are small developed between 500 and 700 m water depth and do not appear to be related to deformation associated with currently subducting seamounts.

a steep middle slope contains normal faults, but with smaller seafloor scarps and are not associated with large failures.

3.5.1. Translational Slides

[37] Unique in the entire study area is a group of translational slides at canyon flanks of the upper slope. About 20 structures of comparable dimensions, <4 km long, <3 km wide, and ~150 m high headwalls occur mostly in a group at 1200–2000 m water depth on the 3°–7° dipping upper slope (Figure 17a). The slides occur in the area of deeply incised submarine canyons. The degree of margin incision by canyons is higher than in the Nicaragua segment (compare Figures 16 and 17). A typical failure is slide 370 (Figure 17b) at the southeast flank of a ridge flanked by two canyons. The slides have no deposits, and failed sediment probably traveled into the canyon and downslope, disintegrating into turbidity currents that may have been deposited in the flatter middle slope or into the trench axis.

3.5.2. Rotational Slumps

[38] A few small rotational slumps occur at the lower slope, near the trench axis. Average dimensions are 1 km length, 2 km width and 100 m high headwalls. Similar to the Nicaragua segment, the headwalls develop at normal faults and the slump scar shape seems influenced by fault geometry (Figure 17a).

3.6. Guatemala Segment

[39] In contrast to the El Salvador segment, the Guatemala slope contains abundant mass wasting structures and pervasive trench-subparallel normal faults (Figures 1 and 18a). In contrast to all other segments, here single, discrete slide scars are rare, slope failures of different morphologies and dimensions overprint each other. Apparently the sediment fails comparatively more frequently, particularly on the steep (up to 17°) middle and lower slope, where the largest failures occur.

[40] Along this segment, classification of some failures as rotational slumps or translational slides is unclear. The pattern of headwalls, and subparallel normal fault fabric are well displayed in the slope angle map (Figure 18d).

3.6.1. Rotational Slumps

3.6.1.1. Slumps Formed at Normal Faults

[41] The middle slope contains abundant slumps, with headwalls that predominantly appear to form

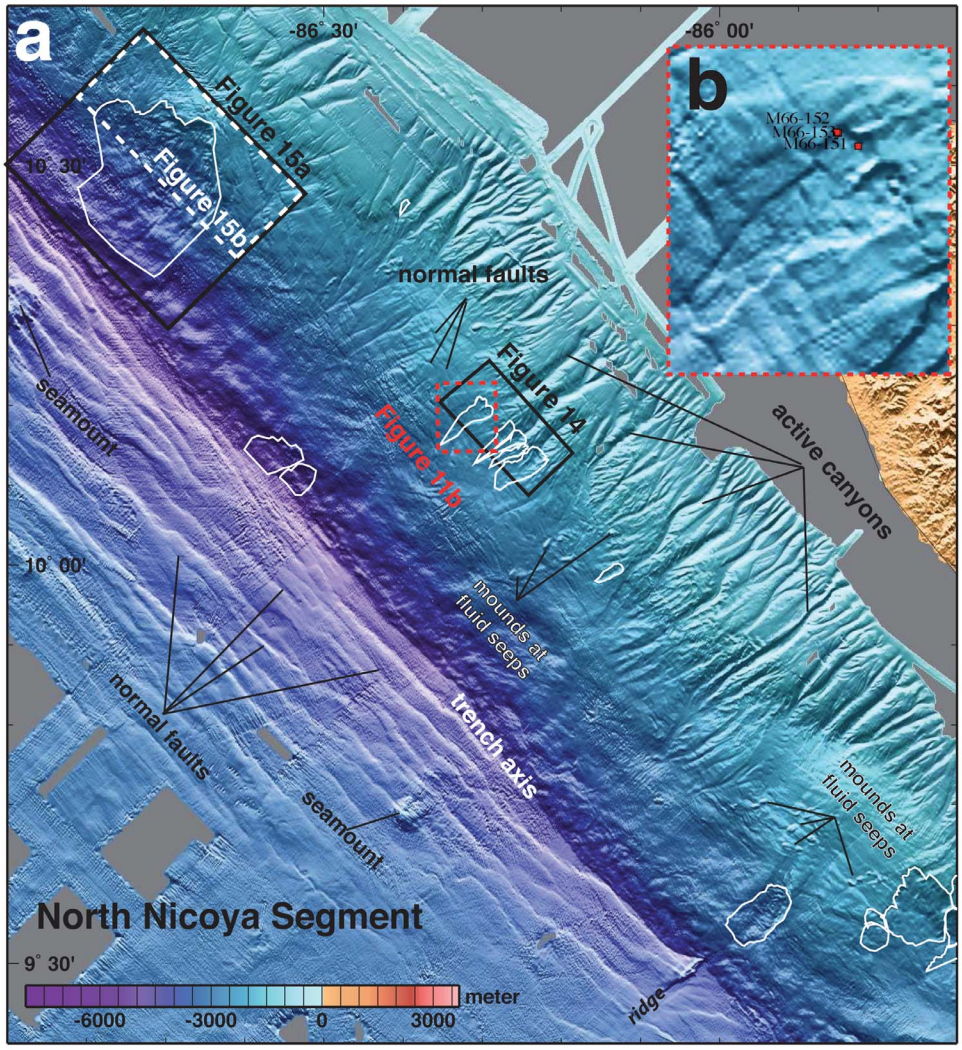

Figure 13. The North Nicoya segment (location in Figure 1a). (a) Shaded relief bathymetric map of the segment. The incoming plate displays the smoothest segment along the study area. The oceanic plate contains few seamounts compared to the SE segment of Costa Rica, and some small- to middle-sized normal faults compared to the segments toward the NW. The continental slope contains comparatively few failures (delineated in white). (b) Shaded relief bathymetric map of a type example of failure: The translational Hermosa slide. Red squares mark location of sediment cores M66-151, M66-152, and M66-153 described in detail by *Harders et al.* [2010]. Numerous scarps parallel to the slope strike indicate that abundant normal faults cut across the area.

at normal fault scarps (Figure 18c). The failure scars are in average 2–8 km long, 5–10 km wide and have 100–300 m high headwalls. Failure planes and sidewalls are short, commonly not well defined, and their downslope extent appears to be controlled by preexisting slope morphology (Figure 18c).

3.6.1.2. Slumps in the Upper Slope

[42] Slumps in the uppermost slope occur where dips are up to 32°. Scars are 1.5–7 km long, 3–8 km wide, and have 100–200 m high headwalls (Figure 18a). The shallow scars show erosional features of younger events obscuring the failure planes. No slump deposits are visible along the steep uppermost slope (Figure 18a).

3.6.1.3. Slumps Formed on the Lowermost Slope

[43] Where the subducting plate displays pronounced horst and graben relief, rotational slumps in the lowermost slope deliver debris into the trench. The thin frontal apex of the overriding plate deforms to mimic the underthrusting horst and

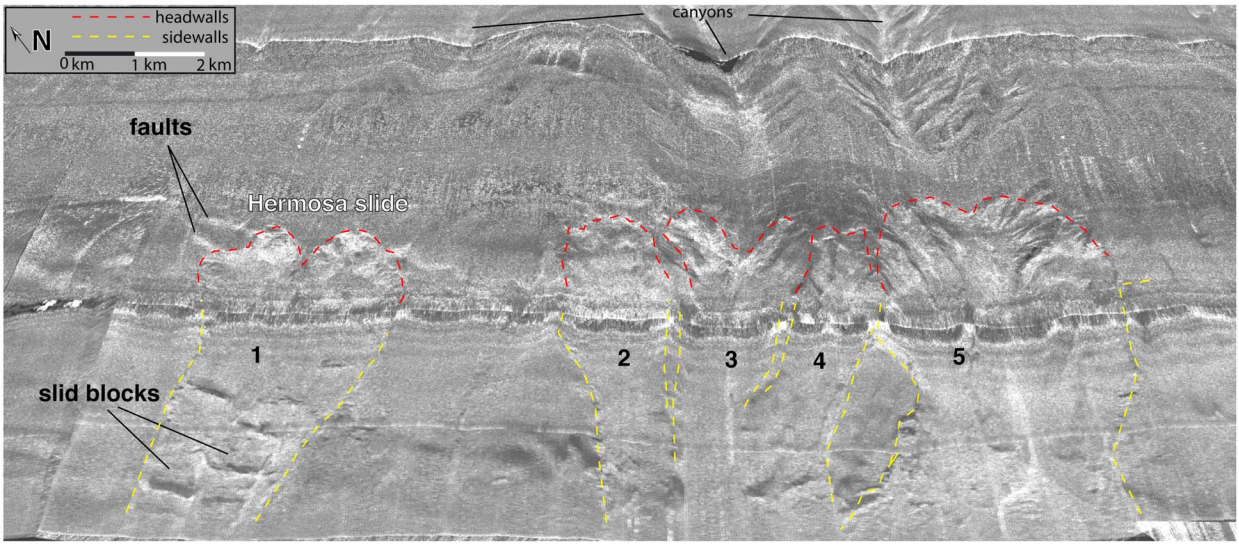

Figure 14. Perspective view of side-scan sonar imagery draped on multibeam bathymetry of a region of the middle slope of the North Nicoya segment (location in Figure 13). The image shows the Hermosa slide and four neighboring slide scars. The slides have formed near the mouth of canyons and where normal faults cut the slope, clearly visible in the northwest part of the headwall of Hermosa slide. Slid blocks are visible on top of the slide plane.

graben topography. This type of slump is most frequent in Guatemala (Figure 18) but with the exception of Costa Rica, it appears in all segments. Their dimensions and shape are similar from Guatemala to North Nicoya, ranging between 1.5 and 3 km long, 3 and 7 km wide, and 300 and 400 m high headwalls (Figures 1, 13a, 16a, 17a, and 18a).

3.6.2. Translational Slides

3.6.2.1. Large Slides Formed on the Lower Slope

[44] In the NW end of the segment, two large translational slides (7–12 km long, 3–5 km wide and 150–300 m high headwalls) are found at water depths >3500 m on the lower slope (Figure 18c). These slides appear to be local features, related to subduction relief of a fracture zone that locally oversteepens the slope (Figure 18b).

3.6.2.2. Slides Linked to Normal Faults Formed Across the Slope

[45] Normal faults slightly oblique to the trench create a rough slope topography. Here develop translational slides with irregular sidewalls and headwalls, and blocky debris deposits downslope (Figure 18a). The shape and lateral extent of failures seem associated with the location and along-strike length of normal faults. In cases, headwall and sidewalls appear to be limited to the extent of fault scarps.

4. Discussion

4.1. Preconditioning Factors

[46] One major question is whether the observed segmentation of the Central American margin, in terms of slide and slump frequency and size (Table 1), may be a function of material properties and/or tectonic setting. An often cited preconditioning are lateral or vertical changes in material properties in the stratigraphic column involved in failures. We have revised previous work on sediment properties along the margin. The slope sediment has been investigated with gravity cores sampling the upper tens of meters offshore Costa Rica and Nicaragua during cruises SO173, M54 and M66 [*Kutterolf et al.*, 2008; *Harders et al.*, 2010]. Also, drill cores from several hundred of meters of slope sediment were taken and analyzed during DSDP Leg 67 offshore Guatemala [*von Huene et al.*, 1980; *Aubouin and von Huene*, 1982], DSDP Leg 84 offshore Guatemala and Costa Rica [*Helm*, 1984], and ODP Leg 170 offshore Costa Rica [*Kimura et al.*, 1997]. It has been proposed that ash layers may act as discontinuity planes in the sediment column and favor formation of detachment planes [*Harders et al.*, 2010]. However, cores show that most of

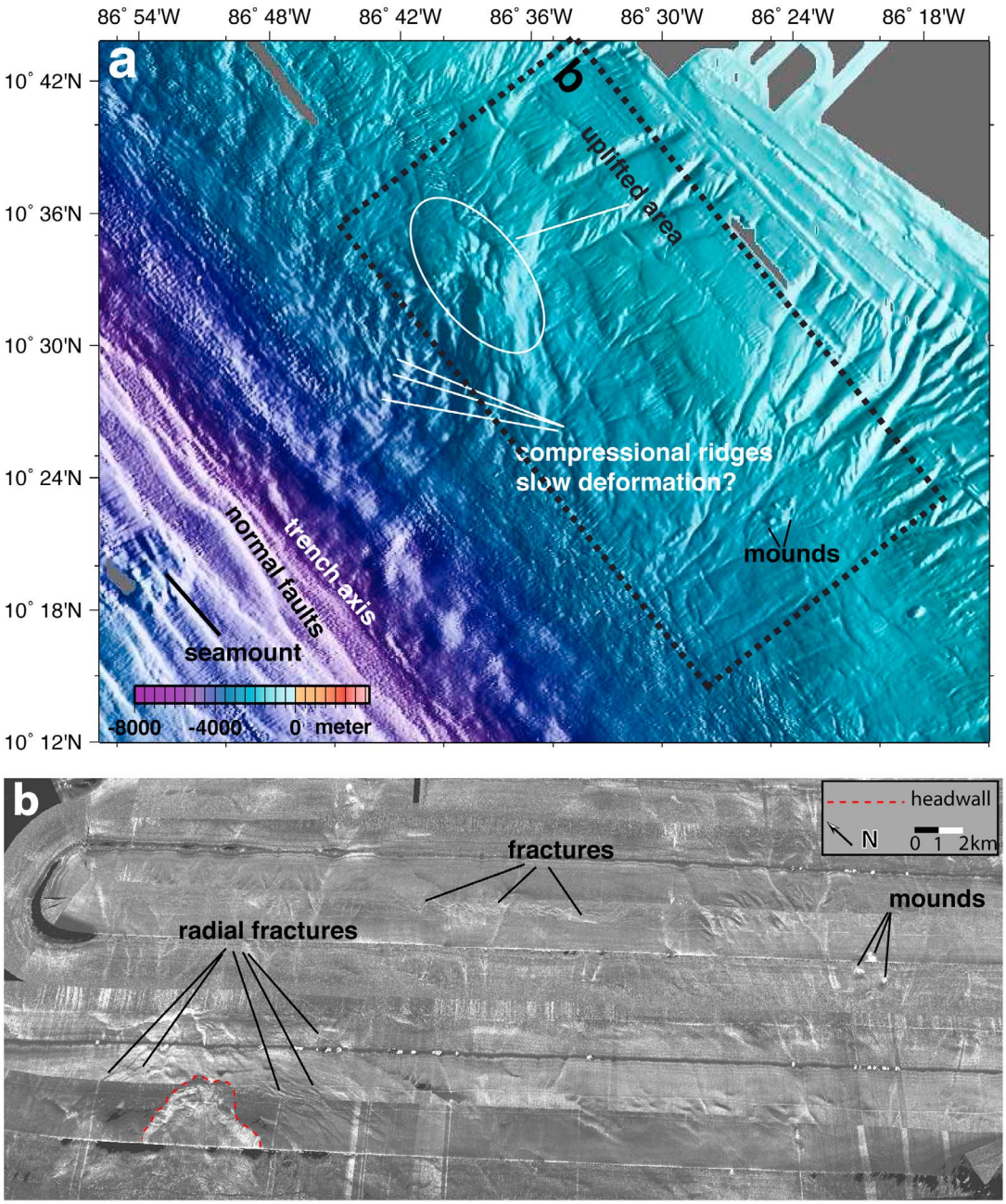

Figure 15. Seafloor maps of the NW region of the North Nicoya segment. (a) Shaded relief bathymetric map showing an uplifted area and, located downslope, a failure scar showing no clear slide sidewalls. Farther downslope occur possible compressional ridges that might indicate slow deformation. (b) Perspective view of side-scan sonar imagery draped on multibeam bathymetry of the middle to upper slope (location in Figure 15a). The image shows the group of radial fractures clustered on the uplifted area and associated headwall. Scarps of discrete normal faults cut the slope at numerous locations.

sediment involved in translational sliding and shallow slumps does not significantly change geographically in any particular property (lithology and stratigraphy, density, water content, and mineralogy). The Pliocene and Pleistocene sediments involved are uniform terrigenous olive green to gray clays, intercalated every few meters by 1–10 cm thick tephra ash layers of the Plinian and ignimbrite eruptions of the Central American Volcanic Arc (DSDP Leg 84 [*Helm*, 1984; *Kutterolf et al.*, 2008]). Typically, bulk densities of the clays increase within the first 200 m from 1.4 to 1.8 g/cm^3 and water

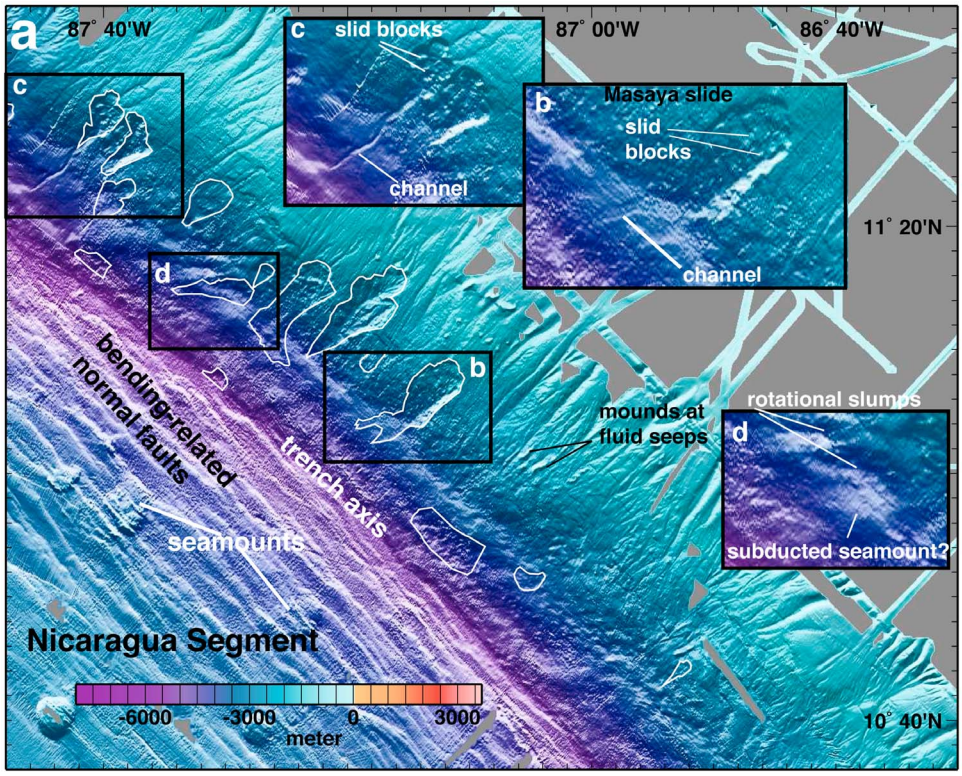

Figure 16. Shaded relief bathymetric map of the Nicaragua segment. (a) The segment displays large translational slides on the middle continental slope and seamounts on the ocean plate that are comparatively smaller than in the Seamounts–Central Costa Rica segment Cocos Ridge–Osa Peninsula segment. (b) Close-up of middle-slope translational Masaya slide showing the slide scar and overlying slid blocks. Failure deposits are missing at the base of the scar. The scar toe converges into a channel that may have been formed by the mass wasting transport processes. (c) Close-up of middle-slope translational slide scars with overlying slid blocks and channel initiating at the scar toe. (d) Close-up of middle- to lower-slope small rotation slumps possibly associated with failure induced by small-scale relief of the incoming oceanic plate.

content reduces between 60 and 30% in response to normal depth-dependent compaction [*von Huene et al.*, 1984]. Therefore, sediment behavior may change with depth from recent sediment to the upper Cretaceous turbidites overlying the igneous basement, but slope sediment stratigraphy does not significantly vary from Guatemala to Costa Rica, probably because the entire region has a similar geological evolution [*Ranero et al.*, 2000]. Further, a succession of dominant marine terrigenous with thin intercalated tephra layers is expected across the entire column since the volcanic arc initiated in the uppermost Cretaceous time [*Ranero et al.*, 2000].

[47] We interpret that long-term tectonic processes cause changes in slope morphology and in the structure of the stratigraphic column [*Ranero et al.*, 2008] that create the most relevant preconditioning factors for slope instability. These factors are combinations of changes in slope dip and upper plate fracturing, both factors caused either locally by subducting topographic features of the ocean plate, or more regionally by tectonic erosion causing normal faulting and oversteepening. Subduction of high-relief features causes slope uplift and oversteepening in the wake of the underthrusting feature, with the locus of oversteepening migrating as the feature moves farther under the margin [*von Huene et al.*, 2000, 2004a, 2004b]. Uplift is also associated with local intense fracturing, that probably cuts across the entire overriding plate [*Ranero and von Huene*, 2000]. These deep penetrating fractures are reactivated during slumping [*von Huene et al.*, 2004a]. Subduction erosion along the underside of the overriding plate removes material that is transferred to the subduction channel and transported away. This process causes gradual thinning of the overriding plate that subsides and extends along normal faults [*Ranero and von Huene*, 2000; *von Huene and Ranero*, 2003]. The intensity

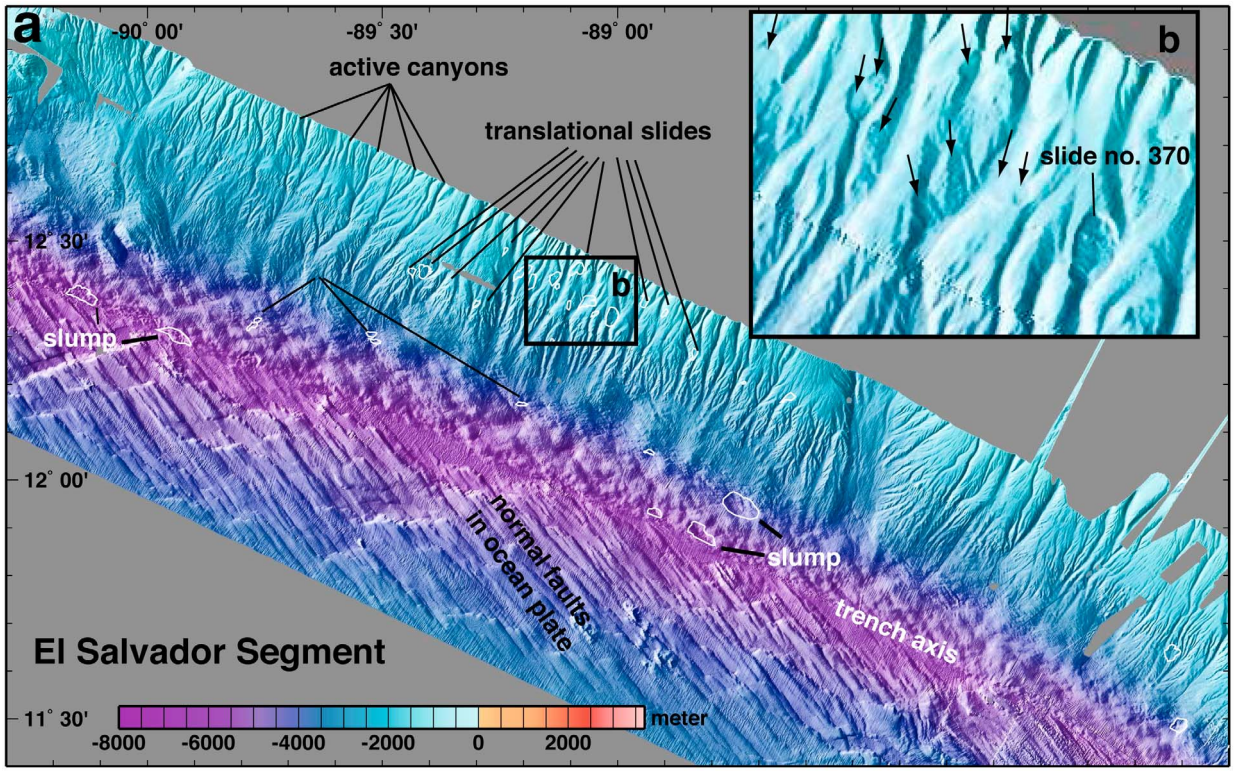

Figure 17. Shaded relief bathymetric map of the El Salvador segment. (a) The segment is characterized by the best developed upper-middle slope canyon system of the study area that possibly implies a comparatively more stable slope. In accord, the segment contains the fewest slope failures of all segments. Typically, these are small translational slides in the upper slope. A few rotational failures seem to initiate at normal fault scarps in the middle to lower slope. A well-developed bending-related normal fault system with large offsets characterize the incoming ocean plate, but no seamounts are present. (b) Close-up of upper slope small translational slides that represent the most abundant type and typically occur at canyon walls.

of erosion appears to change along and across segments, causing differential amount of subsidence and leading to oversteepening typically at the middle slope of some segments and also to variable intensity of faulting that cuts the sediment and in cases the entire overriding plate [*Hensen et al.*, 2004].

[48] El Salvador segment, displays the least active tectonics along the margin, and incision of sediment by canyons in the uppermost slope causes local oversteepening. Oversteepening of canyon walls and intervening ridge flanks may be a preconditioning factor, however of secondary importance in terms of failure abundance and dimensions at a margin dominated by tectonic processes.

[49] The presence of gas hydrates is often cited as a potential preconditioning factor. Gas hydrates, inferred from seismically images bottom simulating reflectors, occur along the margin [*Pecher et al.*, 2001], and might have play a role in small-scale failures in the uppermost slope, but do not explain segmentation.

4.2. Triggering Mechanisms

[50] Trigger mechanisms, understood as the external stimulus that initiates the slope instability process [*Sultan et al.*, 2004], may change for the different segments and failure types. An obvious trigger is gravitational collapse of fractured material in the wake of underthrusting ocean plate relief. This mechanism form slumps in the lowermost slope where hundreds of meters high horst-and-graben relief subducts. This accounts for rotational slumps near the slope toe typically found in Guatemala and El Salvador segments. A similar mechanism has formed the largest rotational slumps in the lower-middle slope of the Seamounts–Central Costa Rica segment. However, seamount subduction under the upper slope of central Costa Rica causes translational sliding. Subduction of comparatively smaller seamounts in Nicaragua produces only translational landslides.

[51] Large subducting seamounts, fracture the entire overriding plate under the middle slope (~5–8 km

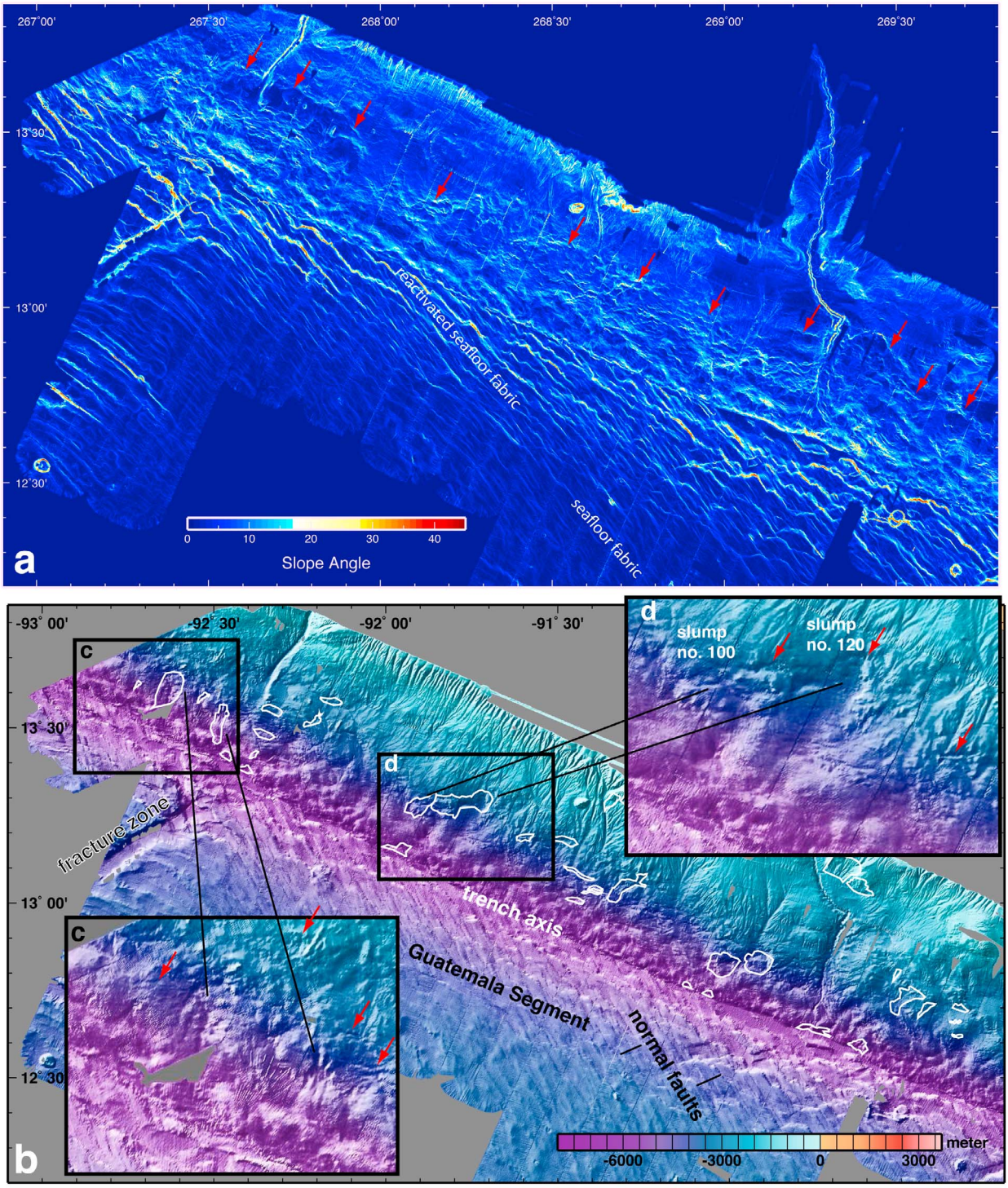

Figure 18. Seafloor maps of the Guatemala segment. (a) Shaded relief bathymetric map of the segment. It displays the greatest variability of types of mass wasting structures of all segments. (b) Local slope angle. The image displays numerous normal fault scarps. Normal faulting initiates in the upper part of the middle slope, indicated by red arrows, and develops across the middle-lower slope, affecting the development and shape of slope failures. The rough topography of the slope possibly indicates a comparatively high frequency of slope failure. (c) Close-up of the lower slope translational slides, which are oriented along fault scarps indicated by arrows. (d) Close-up of the middle slope. Rotational failures with irregular shapes start at or near normal fault scarps indicated by arrows and are difficult to distinguish from faulting scarps.

thick). These fractures will then be the location where deep-rooted detachments of slumps develop [*von Huene et al.*, 2004a]. The slump moves downslope as the seamount underthrusts further, and the previously uplifted area collapses. Examples are Jaco, Parrita and Nicoya slumps. When large seamounts underthrust the upper slope, like offshore Costa Rica, the plate flexes upward, but it is sufficiently thick (~8–12 km thick) not to be broken. Here failure is not along steep scarps, and shallower (few hundred meters thick) translational slides (e.g., Quepos and Cabo Blanco slides) form. In Nicaragua, seismically imaged underthrusted seamounts [*McIntosh et al.*, 2007] have not made a furrow in the slope along their trail, indicating that they do not break the entire overriding plate. Here, sediment fails along strata-parallel detachment planes (e.g., Masaya slide). Rapid oversteepening above subducting topography may trigger translational slides in the upper slope of central Costa Rica and middle slope of the Nicaragua segment.

[52] How failure ultimately evolves during collapse is unclear, and the downslope progress of a landslide may be influenced by a combination of processes including seismicity and fluid flow that may work in conjunction or in a cumulative manner. The largest historical earthquakes in the region are interplate thrusts with magnitude >6, Mw < 8, occurring at depths of 20–30 km, and 50–100 years recurrence time [*Ambraseys and Adams*, 1996]. Several studies indicate that interplate earthquakes of >Mw ~6 occur every 30–50 years along several sectors of each segment. The identified 147 failures include some that contain multiple failures and thus the total failure abundance is somewhat larger. Taking that into account and assuming a linear correspondence between large earthquakes and slides, would suggest that all slides could be created in a few hundreds of years, which appears to be unlikely. We know that the furrow reaching Jaco scar (Figures 4 and 8) has formed in ~230000 years, which is the time required for the seamount to underthrust to its present position assuming current convergence rates. The furrow contains a few slides that suggest a comparatively larger time span for sliding that for large earthquakes. We interpret that if large magnitude earthquakes and slumping occurred at similar rates, there should be more failures. Integrating large intracrustal and bending-related intraplate events would only increase the probability that the two processes occur at different rates. Thus, even though ground acceleration during earthquake rupture may ultimately influence slumping, the rates of both phenomena are dissimilar.

[53] Fluid flow along detachment planes and fracture networks might also play a role. Outflow of deep source fluid originating at the plate boundary and traversing the upper plate has been discovered at many seafloor seepages and fault scarps along the slope of the MAT [*Hensen et al.*, 2004; *Sahling et al.*, 2008; *Ranero et al.*, 2008]. Fluids probably also ascent along seamount subduction induced fractures, and abundant chemosynthetic fauna found on Jaco scarp [*Sahling et al.*, 2008] support that deep-sourced, nutrient-rich fluids ascent along steep detachments.

[54] Translational sliding may be controlled by discrete sediment layers and deformation by faults. Typically the successions contain several meters thick terrigenous turbidites, intercalated by several cm thick ash layers. The ash layers may form weak layers in the sediment column. *Harders et al.* [2010] report that a core taken near the upper headwall area of the translational Hermosa slide recovered the slide plane, identified as a regionally mapped ash layer (Figure 13b). The upper part of the ash layer was removed, leaving only the coarse-grained basal section overlain by marine clays. *Harders et al.* [2010] interpret that the layer experienced liquefaction during earthquake shaking. Liquefaction created a water film sandwiched between clay-rich sediment, promoting translational sliding along the lubricated zone. Cores taken on cruises SO 173, M54, and M66 on the slope from Guatemala to Nicaragua found 5–10 cm thick ash layers intercalated about every 1 m, creating the distinct coarse tephra and clay layering. This makes the mechanism of weak fluid-rich, coarse ash layers (preconditioning) and earthquakes (trigger) viable for translational sliding in the entire area.

[55] Fluids and/or gas from gas hydrate dissociation are often proposed trigger mechanisms. Hydrate dissociation might trigger comparatively small slides in the uppermost slope offshore Costa Rica (Figure 12). These slides occur at ~550 m water depth, near to the upper limit of gas hydrate stability, seismically imaged in this area [*Marquardt*, 2005]. Numerical modeling of degradation of organic matter, using data from cruises M54, SO173 and ODP Leg 140 Site 1041, estimated that in situ formation of methane is insufficient to reach methane saturation in pore water to precipitate gas hydrate, and thus gas hydrate dissociation appears to be unlikely as failure trigger [*Marquardt*, 2005]. However, the spatial correspondence of bottom simulating

reflectors and several slides in the uppermost slope supports a causal relationship, and a role of deeper methane (biogenic or thermogenic) migrating and accumulating upslope cannot be discarded.

[56] Subduction of seamounts and ridges appear to play a major role in slope preconditioning offshore Costa Rica and Nicaragua, and horst and graben relief for slumping in the lower slope of the region. However, other processes probably precondition the middle and upper slope of El Salvador and Guatemala. Offshore El Salvador, normal faulting is relatively subdued and canyons incise the upper slope where they are particularly well developed in comparison to any other segment of the margin, indicating a comparatively tectonically stable segment. Abundant translational slides cut the flanks of carved ridges and canyon flanks. We interpret that these structures result from oversteepening. Progressive incision along long-lived canyons create steep canyon walls that fail in relatively small slides. The unlikely influence of the subducting plate topography on the upper slope appears to indicate that seismic shaking and perhaps fluid outflow at the canyon flanks might be potential triggers. Offshore Guatemala a steep middle-upper slope is cut by numerous slightly trench-oblique normal faults. The result is a hummocky terrain possibly formed by comparatively frequent failures, however failures are considerably smaller that in Nicaragua and Costa Rica. The failures are randomly distributed, have short runout distances and overprint earlier events. The failures seem to predominantly form at normal fault scarps, with broad and short scars extending parallel to the faults. The short runout distances may be due to the hummocky slope morphology that stops failed sediment. We interpret that preconditioning in the Guatemala is dominantly caused by basal tectonic erosion. This process leads to gradual thinning of the overriding plate, associated normal faulting, and progressive steepening of slope sectors. A particular triggering mechanism here is not obvious, and could be any one of the mechanisms discussed above.

5. Conclusions

[57] This work presents the first comprehensive study of mass wasting processes at a continental slope of an extensive section of a convergent margin dominated by subduction erosion. We have detected and analyzed an inventory of 147 failure structures along ~1300 km of the continental slope of the MAT.

[58] We mapped various types of translational slides, more abundant in central Costa Rica, Nicaragua and El Salvador segments. Two types of rotational slumps are related to seamount subduction offshore central Costa Rica and to normal faults in the slope in the Guatemala segment. We identified large rockfalls only along the narrow and steep slope offshore Osa Peninsula, where Cocos Ridge subducts. Other segments like North Nicoya and El Salvador display a comparatively low abundance of failures, and the few failures are relatively small.

[59] The combination of distribution and abundance of failures, and slope width and angle indicates a segmentation of the slope into six regions containing different assemblies of mass-wasting features (Figure 1 and Table 1). Different types of failure usually characterize the lower, middle and upper slope sectors of each segment. We conclude that the variability of structures that define the along-margin segmentation, and across-slope changes primarily reflects variations in tectonic processes, controlled by variations the style and intensity of tectonic erosion, and in deformation related to relief of the oceanic plate. Variations in deformation patterns along and across the slope are possibly related to a first degree to changes in both topography of subducting volcanic constructions (conical seamounts, guyots, ridges), and relief formed by bending-related deformation of the oceanic plate (horst and graben). In support, along-trench changes in character of the oceanic plate exhibit a distribution that corresponds to the interpreted segmentation of the continental slope opposite.

[60] Other preconditioning factors like sedimentation rate, changes in sediment type, and presence of gas hydrate commonly invoked in other settings, do not noticeably change along the strike of the margin, and although may locally be involved in failure, cannot explain the distribution and style of failure.

[61] Gravitational collapse above moving underthrusting relief is a likely failure trigger for slumps. Fast oversteepening above subducting topography may trigger translational slides in the middle slope of Nicaragua or upper slope of Costa Rica. Other possible trigger is earthquake shaking. However, we suggest that the rate of sliding is considerably lower that than recurrence time of large earthquakes (>Mw6). Earthquake magnitude and recurrence time do not appear to be variable enough along the MAT [*Ambraseys and Adams*, 1996] to explain the segmentation of mass-wasting structures.

Acknowledgments

[62] This study is contribution 202 of the Sonderforschungsbereich (SFB) 574 funded by Deutsche Forschungsgemeinschaft (DFG). The data were collected during cruises of German R/V *Sonne* funded by the Ministry of Science and Education (BMBF) and R/V *Meteor* funded by the Deutsche Forschungsgemeinschaft (DFG) and U.S. R/V *M. Ewing* funded by NSF. We acknowledge the journal reviewer comments by J. Chaitor and D. Scholl that helped improve the clarity of the paper.

References

Ambraseys, N. N., and R. D. Adams (1996), Large-magnitude Central American earthquakes, 1898–1994, *Geophys. J. Int.*, *127*, 665–692, doi:10.1111/j.1365-246X.1996.tb04046.x.

Aubouin, J., and R. von Huene (1982), *Initial Reports of the Deep Sea Drilling Project*, vol. 67, Deep Sea Drill. Program, U.S. Gov. Print. Off., Washington, D. C., doi:10.2973/dsdp.proc.67.1982.

Aubouin, J., J. F. Stephan, J. Roump, and V. Renard (1982), The Middle America Trench as an example of a subduction zone, *Tectonophysics*, *86*, 113–132.

Baltuck, M., E. Taylor, and K. McDougall (1985), Mass movement along the inner wall of the Middle America Trench, Costa Rica, *Initial Rep. Deep Sea Drill. Proj.*, *84*, 551–570.

Bialas, J., E. Flueh, and G. Bohrmann (1999), FS SONNE, cruise report SO144/1 and 2PAGANINI; San Diego–Caldera (September 7–November 7, 1999), *Rep. 94*, pp. 1–437, Leibniz Inst. of Mar. Sci. at Univ. of Kiel (IFM-GEOMAR), Kiel, Germany.

Caress, D. W., and D. N. Chayes (1996), Improved processing of Hydrosweep DS multibeam data on the R/V *Maurice Ewing*, *Mar. Geophys. Res.*, *18*, 631–650, doi:10.1007/BF00313878.

DeMets, C., R. G. Gordon, D. F. Argus, and S. Stein (1990), Current plate motions, *Geophys. J. Int.*, *101*, 425–478, doi:10.1111/j.1365-246X.1990.tb06579.x.

Fine, I. V., A. B. Rabinovich, B. D. Bornhold, R. Thomson, and E. A. Kulikov (2005), The Grand Banks landslide-generated tsunami of November 18, 1929: Preliminary analysis and numerical modeling, *Mar. Geol.*, *215*, 45–57, doi:10.1016/j.margeo.2004.11.007.

Flemings, P. B., H. Long, B. Dugan, J. Germaine, C. M. John, J. H. Behrmann, D. Sawyer, and IODP Expedition 308 Scientists (2008), Pore pressure penetrometers document high overpressure near the seafloor where multiple submarine landslides have occurred on the continental slope, offshore Louisiana, Gulf of Mexico, *Earth Planet. Sci. Lett.*, *269*, 309–325, doi:10.1016/j.epsl.2007.12.005.

Hampton, M. A., and H. J. Lee (1996), Submarine landslides, *Rev. Geophys.*, *34*, 33–59, doi:10.1029/95RG03287.

Harders, R., S. Kutterolf, C. Hensen, T. Moerz, and W. Brueckmann (2010), Tephra layers: A controlling factor on submarine translational sliding?, *Geochem. Geophys. Geosyst.*, *11*, Q05S23, doi:10.1029/2009GC002844.

Helm, R. (1984), Mineralogy and diagenesis of slope sediments offshore Guatemala and Costa Rica, Leg 84, *Proc. Deep Sea Drill. Program Initial Rep.*, *15*, 571–594.

Hensen, C., K. Wallmann, M. Schmidt, C. R. Ranero, and E. Suess (2004), Fluid expulsion related to mud extrusion off Costa Rica—A window to the subducting slab, *Geology*, *32*, 201–204, doi:10.1130/G20119.1.

Hühnerbach, V., D. G. Masson, G. Bohrmann, J. M. Bull, and W. Weinrebe (2005), Deformation and submarine landsliding caused by seamount subduction beneath the Costa Rica continental margin—New insights from high-resolution sidescan sonar data, in *Submarine Slope Systems: Processes and Products*, edited by D. M. Hodgons and S. S. Flint, *Geol. Soc. Spec. Publ.*, *244*, 195–205.

Johnson, D. W. (1939), Origin of submarine canyons, *J. Geol.*, *2*, 42–60, 133–158, 213–236.

Kimura, G., E. Silver, P. Blum, and the Leg 170 Scientific Party (1997), *Proceedings of the Ocean Drilling Program, Initial Reports*, vol. 170, Ocean Drill. Program, College Station, Tex.

Kukowski, N., J. Greinert, and S. Henrys (2010), Morphometric and critical taper analysis of the Rock Garden region, Hikurangi Margin, New Zealand: Implications for slope stability and potential tsunami generation, *Mar. Geol.*, *272*, 141–153, doi:10.1016/j.margeo.2009.06.004.

Kutterolf, S., A. Freundt, W. Peréz, T. Mörz, U. Schacht, H. Wehrmann, and H.-U. Schmincke (2008), Pacific offshore record of plinian arc volcanism in Central America: 1. Along-arc correlations, *Geochem. Geophys. Geosyst.*, *9*, Q02S01, doi:10.1029/2007GC001631.

Locat, J., and H. J. Lee (2002), Submarine landslides: Advances and challenges, *Can. Geotech. J.*, *39*, 193–212, doi:10.1139/t01-089.

Marquardt, M. (2005), Investigation of a submarine landslide off Costa Rica: Reconstruction of the date and the sedimentary and geochemical development of the BGR-landslide, diploma thesis, Inst. of Geosci., Fac. of Math. and Nat. Sci., Christian-Albrechts-Univ. of Kiel, Kiel, Germany.

McAdoo, B. G., L. F. Pratson, and D. L. Orange (2000), Submarine landslide geomorphology, US continental slope, *Mar. Geol.*, *169*, 103–136, doi:10.1016/S0025-3227(00)00050-5.

McIntosh, K. D., E. A. Silver, I. Ahmed, A. Berhorst, C. R. Ranero, R. K. Kelly, and E. R. Flueh (2007), The Nicaragua Convergent Margin: Seismic reflection imaging of the source of a tsunami earthquake, in *The Seismogenic Zone of Subduction Thrust Faults*, edited by T. Dixon and J. C. Moore, pp. 257–287, Columbia Univ. Press, New York.

Mienert, J., J. Posewang, and M. Baumann (1998), Gas hydrates along the northeastern Atlantic margin: Possible hydrate-bound margin instabilties and possible release of methane, in *Gas Hydrates: Relevance to World Margin Stability and Climatic Change*, edited by J.-P. Henriet and J. Mienert, *Geol. Soc. Spec. Publ.*, 137, 275–291.

Mulder, T., and P. Cochonat (1996), Classification of offshore mass movements, *J. Sediment. Res.*, *66*, 43–57.

Orange, D., and N. Breen (1992), The effects of fluid escape on accretionary wedges: 2. Seepage force, slope failure, headless submarine canyons, and vents, *J. Geophys. Res.*, *97*(B6), 9277–9295, doi:10.1029/92JB00460.

Pecher, I., N. Kukowski, C. R. Ranero, and R. von Huene (2001), Gas hydrates along the Peru and Middle America Trench systems, in *Natural Gas Hydrates: Occurrence, Distribution, and Detection*, *Geophys. Monogr. Ser.*, vol. 124, pp. 257–271, AGU, Washington, D. C.

Ranero, C. R., and R. von Huene (2000), Subduction erosion along the Middle America convergent margin, *Nature*, *404*, 748–752, doi:10.1038/35008046.

Ranero, C. R., R. von Huene, E. Flueh, M. Duarte, D. Baca, and K. McIntosh (2000), A cross section of the convergent Pacific margin of Nicaragua, *Tectonics*, *19*(2), 335–357, doi:10.1029/1999TC900045.

Ranero, C. R., A. Villaseñor, J. Phipps Morgan, and W. Weinrebe (2005), Relationship between bend-faulting at trenches and intermediate-depth seismicity, *Geochem. Geophys. Geosyst.*, *6*, Q12002, doi:10.1029/2005GC000997.

Ranero, C. R., I. Grevemeyer, H. Sahling, U. Barckhausen, C. Hensen, K. Wallmann, W. Weinrebe, P. Vannucchi, R. von Huene, and K. McIntosh (2008), The hydrogeological system of erosional convergent margins and its influence on tectonics and interplate seismogenesis, *Geochem. Geophys. Geosyst.*, *9*, Q03S04, doi:10.1029/2007GC001679.

Ratzov, G., M. Sosson, J.-Y. Collot, S. Migeon, F. Michaud, E. Lopez, and Y. Le Gonidec (2007), Submarine landslides along the North Ecuador–South Colombia convergent margin: Possisible tectonic control, in *Submarine Mass Movements and Their Consequences*, edited by V. Lykousis, D. Sakellariou, and J. Locat, pp. 47–55, Springer, Dordrecht, Netherlands, doi:10.1007/978-1-4020-6512-5_6.

Sahling, H., D. G. Masson, C. Ranero, V. Hühnerbach, W. Weinrebe, I. Klaucke, D. Bürk, W. Brückmann, and E. Suess (2008), Fluid seepage at the continental margin offshore Costa Rica and southern Nicaragua, *Geochem. Geophys. Geosyst.*, *9*, Q05S05, doi:10.1029/2008GC001978.

Sawyer, D. E., P. B. Flemings, R. C. Shipp, and C. D. Winker (2007), Seismic geomorphology, lithology, and evolution of the late Pleistocene Mars-Ursa turbidite region, Mississippi Canyon area, northern Gulf of Mexico, *AAPG Bull.*, *91*, 215–234, doi:10.1306/08290605190.

Skempton, A. W., and J. N. Hutchinson (1969), Stability of natural slopes and embankment foundations: State-of-the-art report, paper presented at 7th International Conference on Soil Mechanics and Foundation Engineering, Soc. Mex. de Mec. de Suelos Mex., Mexico City.

Sultan, N., et al. (2004), Triggering mechanisms of slope instability processes and sediment failures on continental margins: A geotechnical approach, *Mar. Geol.*, *213*, 291–321, doi:10.1016/j.margeo.2004.10.011.

Tappin, D. R., P. Watts, G. M. McMurtry, Y. Lafoy, and T. Matsumoto (2001), The Sissano, Papua New Guinea tsunami of July 1998—Offshore evidence on the source mechanism, *Mar. Geol.*, *175*, 1–23, doi:10.1016/S0025-3227(01)00131-1.

Vannucchi, P., C. R. Ranero, S. Galeotti, S. M. Straub, D. W. Scholl, and D. McDougall-Ried (2003), Fast rates of subduction erosion along the Costa Rica Pacific margin: Implications for nonsteady rates of crustal recycling at subduction zones, *J. Geophys. Res.*, *108*(B11), 2511, doi:10.1029/2002JB002207.

Vannucchi, P., S. Galeotti, P. Clift, C. R. Ranero, and R. von Huene (2004), Long term subduction erosion along the Middle America Trench offshore Guatemala, *Geology*, *32*, 617–620, doi:10.1130/G20422.1.

von Huene, R., and C. R. Ranero (2003), Subduction erosion and basal friction along the sediment-starved convergent margin off Antofagasta, Chile, *J. Geophys. Res.*, *108*(B2), 2079, doi:10.1029/2001JB001569.

von Huene, R., et al. (1980), Leg 67: The Deep Sea Drilling Project Mid-America Trench transect off Guatemala, *Geol. Soc. Am. Bull.*, *91*(7), 421–432, doi:10.1130/0016-7606(1980)91<421:LTDSDP>2.0.CO;2.

von Huene, R., et al. (1984), *Proceedings of the Deep Sea Drilling Program, Initial Reports*, vol. 84, U.S. Gov. Print. Off., Washington, D. C.

von Huene, R., J. Bourgois, J. Miller, and G. Pautot (1989), A large tsunamogenic landslide and debris flow along the Peru Trench, *J. Geophys. Res.*, *94*(2), 1703–1714, doi:10.1029/JB094iB02p01703.

von Huene, R., C. R. Ranero, W. Weinrebe, and K. Hinz (2000), Quaternary convergent margin tectonics of Costa Rica, segmentation of the Cocos Plate, and Central American volcanism, *Tectonics*, *19*, 314–334, doi:10.1029/1999TC001143.

von Huene, R., C. R. Ranero, and P. Watts (2004a), Tsunamigenic slope failure along the Middle America Trench in two tectonic settings, *Mar. Geol.*, *203*, 303–317, doi:10.1016/S0025-3227(03)00312-8.

von Huene, R., C. R. Ranero, and P. Vanucchi (2004b), Generic model of subduction erosion, *Geology*, *32*, 913–916, doi:10.1130/G20563.1.

Weinrebe, R. W., and E. R. Flueh (2002), Cruise report SO163—Subduction I internal report, *Contrib. 14*, SFB 574, Leibniz Inst. of Mar. Sci. at Univ. of Kiel (IFM-GEOMAR), Kiel, Germany.

Weinrebe, R. W., and C. R. Ranero (2004), Cruise report SO173/2 "Seduction"—Seismogenesis and tectonic erosion during subduction: Middle America Margin internal report, *Contrib. 48*, SFB 574, Leibniz Inst. of Mar. Sci. at Univ. of Kiel (IFM-GEOMAR), Kiel, Germany.

Werner, R., K. Hoernle, P. van den Bogaard, C. Ranero, R. von Huene, and D. Korich (1999), Drowned 14-m.y.-old Galápagos archipelago off the coast of Costa Rica: Implications for tectonic and evolutionary models, *Geology*, *27*, 499–502, doi:10.1130/0091-7613(1999)027<0499:DMYOGP>2.3.CO;2.

Wessel, P., and W. H. F. Smith (1998), New improved version of generic mapping tools released, *Eos Trans. AGU*, *79*, 579, doi:10.1029/98EO00426.

Wilson, D. S. (1996), Fastest known spreading on the Miocene Cocos-Pacific plate boundary, *Geophys. Res. Lett.*, *23*, 3003–3006, doi:10.1029/96GL02893.